DUDLEY KNOX LIBRARY
NAVAL POSTGRADUATE SCHOOL
MONTEREY, CALIFORNIA 93943-5002

The Pennsylvania State University

The Graduate School

Department of Nuclear Engineering

NEUTRON IRRADIATION EFFECTS ON THE MECHANICAL PROPERTIES OF HY-80 STEEL

A Paper in

Nuclear Engineering

by

William F. Nold

Submitted in Partial Fulfillment

of the Requirements

for the Degree of

Master of Engineering

December 1986

I grant the Pennsylvania State University the nonexclusive right to use this work for the University's own purposes and to make single copies of the work available to the public on a not-for-profit basis if copies are not otherwise available.

Abstract

HY-80 steel is a high strength steel used by the U. S. Navy in constructing nuclear submarine hulls. Although not used in reactor component construction, the need to know the effects of neutron irradiation on its mechanical properties is evident because the steel will acquire a fast neutron dose over the lifetime of the vessel. Additionally, future construction of reactor vessels and components is expected to rely, to a higher degree, on the use of these high strength steel alloys.

The mechanical properties of HY-80 steel is affected by neutron irradiation when bombarding neutrons collide with the material's atomic structure. Radiation defects caused by this damage then hinder or prevent dislocation movement through the structure, which in turn "hardens" the steel.

Previous research on this subject has concluded that irradiation levels on the order of 3×10^{19} n/cm^2 can increase the steel's strength by as much as 50%, and raise its ductile-brittle transition temperature several hundred degrees. Few previous studies have shown measurable effects on the mechanical properties of HY-80 steel if irradiation levels are below 1×10^{18} n/cm^2.

The research discussed in this paper did find that irradiation levels of 5×10^{17} n/cm^2 do result in measurable effects on the strength and hardness of HY-80 steel, and that increasing irradiation fluence levels increases the magnitude of these effects.

We approve this paper of William F. Nold.

Date of Signature:

Table of Contents

Page

Title.....i

Abstract.....ii

Signature page.....iii

Table of Contents.....iv

List of Figures.....v

List of Tables.....viii

Acknowledgements.....x

I. INTRODUCTION.....1

II. THE DAMAGE MECHANISM.....6

III. THE EFFECTS ON MECHANICAL PROPERTIES.....19

IV. PREVIOUS RESEARCH ON HY-80 STEEL.....40

V. EXPERIMENTAL DESCRIPTION AND RESULTS.....66

VI. CONCLUSIONS 82

References.....83

List of Figures

		Page
Figure 1	A spike of displaced atoms (x) and vacancies (o) (Ref. [4])	11
Figure 2	Original version of a displacement spike (Ref. [2])	12
Figure 3	Later version of a displacement spike (Ref. [2])	12
Figure 4	Sequence of focussed collisions (Ref. [4])	14
Figure 5	Schematic diagram of the damage mechanism in a neutron-irradiated solid (Ref. [8])	16
Figure 6	Representative Stress-strain curves (Ref. [2,10])	21
Figure 7	Stress-strain diagram for a ductile steel (Ref. [10])	23
Figure 8	Stress-strain curves showing toughness (Ref. [11])	25
Figure 9	Ductile-brittle transition (Ref. [4])	27
Figure 10	Formation of dendrites (a) leading to a polycrystalline structure (b) (Ref. [4])	29
Figure 11	Grain-boundary models: (a) Large-angle grain boundary (b) Small-angle grain boundary (Ref. [2])	30
Figure 12	Edge dislocation lattice defect caused by introduction of extra half plane of atoms (Ref. [11])	31

Figure 13 The screw dislocation (Ref. [2]).....32

Figure 14 Plastic deformation of a single crystal (Ref. [2]).....33

Figure 15 Slip planes and slip direction in bcc crystals (Ref. [2]).....33

Figure 16 Transition temperature shift resulting from neutron-irradiation (Ref. [11]).....36

Figure 17 Effect of fast neutron fluence on the increase in the nil-ductility-temperature (Ref. [2]).....37

Figure 18 Effect of fast neutron irradiation on the tensile properties of reactor steels (Ref. [2]).....38

Figure 19 Relationship of initial NDT of various steels to reactor startup and operating temperatures (Ref. [13]).....43

Figure 20 Increase in the NDT resulting from irradiation below 450°F (Ref. [3]).....44

Figure 21 Effect of neutron radiation on the notch-toughness of carbon and alloy steels irradiated below 500°F (Ref. [3]).....45

Figure 22 Increase in the NDT resulting from irradiation at higher temperatures (Ref. [3]).....46

Figure 23 Transition temperature shifts resulting from elevated temperature irradiation of HY-80 steel (Ref. [14]).....47

Figure 24 Yield strength increases of carbon and alloy steels after irradiation to 500°F (Ref. [3]).....50

Figure 25 The tensile properties of HY-80 steel to 750°F for the indicated irradiation conditions (Ref. [15]).....52

Figure 26 DBTT changes of HY-80 steels as compared to trends established by NRL and by Carpenter (Ref. [18]).....57

Figure 27 Charpy V-notch ductility characteristics of the high strength 7.5Ni-Cr-Mo steel before and after irradiations to two neutron exposure levels at a temperature of 280°F (Ref. [21]).....59

Figure 28 Charpy V-notch ductility characteristics of three steels of different strength levels after simultaneous irradiations at 550°F (Ref. [21]).....62

Figure 29 Dimensions for hardness specimen.....67

Figure 30 Specifications for tensile specimen (Ref. [22]).....68

Figure 31 Specifications for impact test specimen (Ref. [22]).....68

Figure 32 Tube A irradiation arrangement.....70

Figure 33 Tube A shielding design.....71

Figure 34 Tube B irradiation arrangement.....72

Figure 35 Tube B shielding design.....73

Figure 36 Sulfur tablet arrangement in Tube B.....74

List of Tables

		Page
Table 1	Composition of HY-80 and A302-B Steel (%)	41
Table 2	Comparison of recovery characteristics of HY-80 and A302-B steels irradiated at 540° and 640°F (Ref. [2,14])	48
Table 3	Ductile-brittle transition temperature for HY-80 and A302-B steel as determined by Charpy V (30 Ft.Lb.) (Ref. [14])	49
Table 4	Tensile properties of HY-80 steel (Ref. [3,17])	51
Table 5	Check analyses of HY-80 specimens tested (Ref. [18])	54
Table 6	Results of pre- and postirradiation tension test at room temperature (Ref. [18])	55
Table 7	Results of pre- and postirradiation Charpy V-notch impact tests (Ref. [18])	55
Table 8	Chemical composition of 3.5Ni-Cr-Mo and 7.5Ni-Cr-Mo steels (in percent) (Ref. [21])	58
Table 9	Mechanical properties of some Ni-Cr-Mo steels (Ref. [21])	59
Table 10	Comparative embrittlement of several steels irradiated simultaneously at <250°F based on Charpy V-notch tests (Ref. [21])	61
Table 11	Charpy V-notch ductility characteristics of several steels irradiated simultaneously at 550°F to 3.8 X 10^{19} n/cm² (Ref. [21])	63

Table 12 Fast neutron flux in Sample Tube B.....74

Table 13 Irradiation summary of the HY-80 samples...75

Table 14 Results of tensile testing.....77

Table 15 Results of hardness testing.....78

Table 16 Results of Charpy V-notch impact testing...78

Acknowledgements

The author wishes to thank Dr. Anthony J. Baratta for his guidance, assistance and encouragement in the preparation of this paper and the staff of the Breazeale Nuclear Reactor for their support and assistance in the research that took place at the reactor. He also wishes to thank Dr. Stephen K. Liu and Dr. Richard A. Queeney of the Industrial Engineering Department for their support and the use of their mechanical testing equipment.

A special thanks goes to the David Taylor Naval Ships Research and Development Center in Annapolis, Maryland for providing the HY-80 steel used in this research.

I. INTRODUCTION

Since the harnessing of the atom and the advent of nuclear power for peaceful purposes in electrical generating stations and propulsion plants, the effects of radiation on the structural materials that make up the reactor plants has played an important part in the design and construction of these nuclear reactors. It has long been known that irradiation alters the physical and mechanical properties of materials. For example, tests by various researchers over the years have shown that an accumulated dose on the order of 3×10^{19} n/cm^2 can increase a steel's yield strength by as much as 50%, and raise its ductile to brittle transition temperature by as much as 200°F. When mechanical properties can be altered this much, the reasons behind the changes must be known. If the plant design engineers expect to do a good job of designing the plant and specifying material that will stand up to these irradiation effects, it is paramount that they understand in as much detail as possible how the nuclear radiation changes the properties of metals and alloys. They must also understand how much damage is done per unit of exposure of radiation and how this might change under varying conditions such as different temperatures or different chemical environments.

The physical properties of a material that can be affected by nuclear radiation include density, elastic constants, stored energy, electrical resistivity, thermal conductivity, thermoelectric effect, and coefficient of

thermal expansion. Mechanical properties that are affected by nuclear radiation include tensile strength, hardness, impact resistance, creep resistance, stress rupture failure, and fatigue.

The damage that leads to the effects on these various physical properties is initiated by interaction between energetic subatomic particles and the components atomic structure. In terms of damage producing capabilities the most important nuclear particles are fission fragments and fast neutrons. Fission fragments are only pertinent within the fuel material itself while neutrons, due to their wide energy spectrum and ability to travel relatively large distances, are pertinent to all the reactor structural materials. Other energetic subatomic particles such as electrons, protons, alpha particles, and gamma rays, can also initiate damage in various materials; however, their contribution to the total damage is negligible when compared with fission fragments and neutrons. In regard to structural materials, the design engineer is mainly interested in the effects of neutron radiation on its mechanical properties.

Considerable work and studies have been conducted on the effects on fuel materials, fuel cladding materials, structural materials used within the pressure vessel and primary systems, and on the various materials used to construct the reactor pressure vessel itself. Not only must the pressure vessel contain the high pressures normally found within a reactor, but it must also withstand numerous

other stresses caused by plant transients, system hydrostatic tests, and plant cooldowns and heatups. Additionally, because it will accumulate a large neutron dose over the lifetime of the reactor, its ability to withstand these stresses, absorb the effects of this irradiation, and still safely contain the system is of utmost importance in reactor design. Consequently, those materials and alloys used in reactor vessel construction have been extensively tested and evaluated. Less thoroughly tested have been those materials that receive much less radiation than the pressure vessel, but, nevertheless, still accumulate a neutron dose over the lifetime of the reactor. A prime example of this is the material used in constructing the pressure hull of a nuclear submarine. This material must be extremely strong, tough, and ductile in order to withstand the pressures of deep submergence and the possibilities of battle damage. That portion of the hull that surrounds the reactor compartment will, over the lifetime of the vessel, accumulate some total dose of neutron radiation.

The material presently being used by the U. S. Navy in constructing nuclear submarine hulls is called HY-80 steel, conforming to Military Specification, MIL-S-16216J(SH) of 10 April 1981 for "Steel Plate, Alloy, Structural, High Yield Strength (HY-80 and HY-100)". As previously mentioned, the U. S. Navy primarily uses these high strength steels in the hulls of combatant ships and for other critical structural applications where a notch-tough, high

strength material is required.

The expected lifetime of a submarine hull is about thirty years. It is the Navy's present policy that during this lifetime, the hull will not receive in excess of 10^{17} nvt or neutron fluences, [1]. By keeping total fast neutron fluences under this level the Navy does not expect to see any detrimental effects on the mechanical properties of the hull due to this irradiation. Consequently, the primary and secondary shielding of the reactor plants are designed to ensure that total doses received by the ship's hulls are less than this figure.

The remainder of this paper is divided into the following sections:

II. The Damage Mechanism

III. The Effect on Mechanical Properties

IV. Previous Research on HY-80 Steel

V. Experimental Research and Results

VI. Conclusions

In Section II, the basic damage mechanism in steels will be examined. This paper will not attempt to explain or describe many of the technical and engineering aspects of the damage mechanism. There are many excellent references available, such as reference [2] to this paper, that cover these aspects in great detail. This paper will only cover some of the basic theories so that the reader will have a minimum understanding of radiation damage in order to better understand the resultant effects that it has on the mechanical properties of HY-80 steel.

In Section III, the tests that are done to evaluate a metal's mechanical properties are discussed, followed by how radiation damage affects these properties.

Section IV will cover previous research that has been conducted on neutron irradiation of HY-80 steel. The results of these studies and how the physical properties are changed will be discussed.

Section V will discuss the research conducted by the author on HY-80 steel at the Pennsylvania State University's Breazeale Nuclear Reactor. It will look at how fast neutron fluences on the order of 5×10^{17} and 1×10^{18} n/cm^2 affect the tensile, impact, and hardness properties of irradiated samples of HY-80 steel. The experimentation conducted in this research was not all inclusive and included only a relatively small number of samples that were subsequently mechanically tested at only one temperature. Consequently, accurate estimates in the shifts of the ductile-brittle transition temperature are not possible, nor is a full analysis of the effects on the irradiated samples possible. However, the experiment should show whether the expected change or trend in the change of mechanical properties does occur as a result of the neutron irradiations. Experimental results do indicate a trend of increasing strength and hardness with increasing neutron fluence.

In Section VI, the author will present conclusions drawn from the paper.

II. THE DAMAGE MECHANISM

This section discusses how damage occurs in metal, and covers the basic damage mechanism from the atomic collision to how the defects congregate to form clusters or depleted zones. It also covers recombination and recovery due to annealing.

Orlander, [2], defines radiation damage as the primary, microscopic events that precede the appearance of gross changes in the solid. Radiation effects, on the other hand, are those macroscopic, observable, and often technologically crucial results of exposure of solids to energetic particles. In other words, the defects in solids caused by radiation damage produce the radiation effects. The difference between radiation damage and radiation effects can also be compared on a time scale. The initial collision between an energetic particle and an atom in a solid can be over in less than 10^{-11} seconds, and the resultant damage can be over in less than 10^{-3} seconds. Radiations effects; however, can take much longer periods of time. Radiation effects are not seen until a substantial amount of damage has occurred. Thus, depending on the growth rate of interstitial defects into clusters and depleted zones which cause the effects, it can take weeks or even months before measurable changes in the mechanical properties can be seen.

The study of radiation damage is, in itself, an exhaustive and intensive field on which numerous volumes of

literature has been written. In thorough studies the analyst will not only try to determine how the damage occurs, but he will also try to predict the number and types of defects occuring in the material, and how these defects will affect the material's properties. A comprehensive study such as this involves the physics of atomic collisions, the mathematics of probability theory, the engineering of nuclear science, the science of metallurgy, and many other disciplines, as well as the ability to tie these fields together and use the information to produce computer models designed to simulate radiation damage. Numerous models and computer codes have been developed over the years that do just that, and the majority of them support the basic concepts of radiation damage that will be covered in this paper.

The major damage mechanism is the atomic collision between an energetic atom or subatomic particle and the structural atoms of the material or the different solute atoms of the alloying elements. The critical event is the collision between the particle and the atom. Upon this collision two events are then possible: a) the particle is captured by the atom, resulting in transmutation, or b) elastic type collision of the particle with the nuclei of the material. Neutrons can produce both such effects. Trudeau, [3]; however, points out that the transmutation effects from neutron capture have negligible effects on the mechanical properties. For example, for most iron isotopes, which are converted to heavier isotopes of iron when

transmutated, in a thermal flux of 10^{11} neutrons/cm^2/sec the transmutation rate is about 0.00001% per year. For a fast flux, where the absorption cross section is even less, the transmutation rate is negligible.

Elastic type collisions by energetic neutrons, therefore, are the major source of the radiation damage in reactor structural materials. These collisions can be crudely compared to a single billiard ball smashing into an ordered lattice of balls on a billiard table. Energetic neutrons, or fast neutrons, are those neutrons that have sufficient energy to cause atomic displacements. In ferritic steel, atoms are arranged in a body-centered-cubic (bcc) lattice. The energy, E_d, required to knock an atom irreversibly out of its site inside the lattice is comparable to, but larger than its binding energy. A. H. Cottrell, [4], reports that both theory and experiment has shown that, typically, E_d is about 25 ev. To impart a recoil energy of 25 ev to an iron atom, the much lighter neutron must have an energy of about 360 ev, [3]. Fast neutrons are generally defined as those over the threshold energy of 1 Mev. Thus, all fast neutrons have more than sufficient energy to cause radiation damage. A direct hit by a 1 Mev neutron would impart about 60,000 ev of recoil energy to an iron atom, [3]. This is obviously more than enough to violently disrupt the atomic lattice, resulting in additional displaced atoms and considerable vibration as the energy dissipates.

A displaced atom in a crystal lattice is known as a point defect. The initial atom, displaced by the neutron, is known as the primary knock-on atom or PKA. The collection of point defects created by a single PKA is known as a displacement cascade. Orlander, [2], points out that one of the earliest and simplest theories on displacement cascades was proposed by Kinchin and Pease, [7]. Their analysis is based on the following assumptions:

1. The cascade is created by a sequence of two body elastic collisions between atoms.

2. The probability of displacement is given by the following equations.

$P(D) = 0$ (for $E < E_d$)

$P(D) = 1$ (for $E > E_d$)

- where E is the energy imparted to the collision atom by the incoming neutron.

- E_d is the displacement threshold energy.

3. The energy E_d consumed in displacing an atom is neglected in the energy balance of the binary collision that transfers kinetic energy to the struck atom.

4. Energy loss by electron stopping is treated by the cutoff energy of the following equation.

$E_c = 10^3 * M_1$ (ev), where M_1 is the mass of the atom.

- If the PKA energy is greater than E_c, then no displacements occur until electronic energy losses reduce the PKA energy to E_c. For all energies less than E_c,

electronic stopping is ignored, and only atomic collisions take place.

5. The energy transfer cross section is given by the hard sphere model.

6. The arrangement of the atoms in the solid is random; effects due to crystal structure are neglected.

The PKA, after it has been initially displaced, recoils through the lattice as a fast moving ion. The PKA, being an iron atom and because of its electrically charged nucleus, interacts with the electrons of the atoms which it passes. The PKA loses energy through this electron interaction as long as its energy is greater than E_c. This energy imparted to the electrons is rapidly converted into heat with little or no permanent damage done to the metal. The PKA continues on until its energy is less then E_c, at which time it will now interact with other atoms through direct collisions. This will continue until the PKA dissipates all of its energy and it comes to rest, crowded into the interstices between the other atoms in the lattice. It may also come to rest in the vacancy site left by another atom. The vacant lattice site that is left behind by each interstitial atom is called a vacancy. Vacancy-interstitial pairs are often called Frenkel defects or pairs. Frenkel defects can cause changes in both the mechanical and physical properties of the material.

A displacement spike results when the PKA atom and all subsequent recoiled atoms in the collision cascade have dissipated all of their energies and have become

interstitials in the metal. Figure 1 shows a simple diagram of a basic displacement spike. This displacement spike model was first introduced by Brinkman, [5], in the mid 1950s.

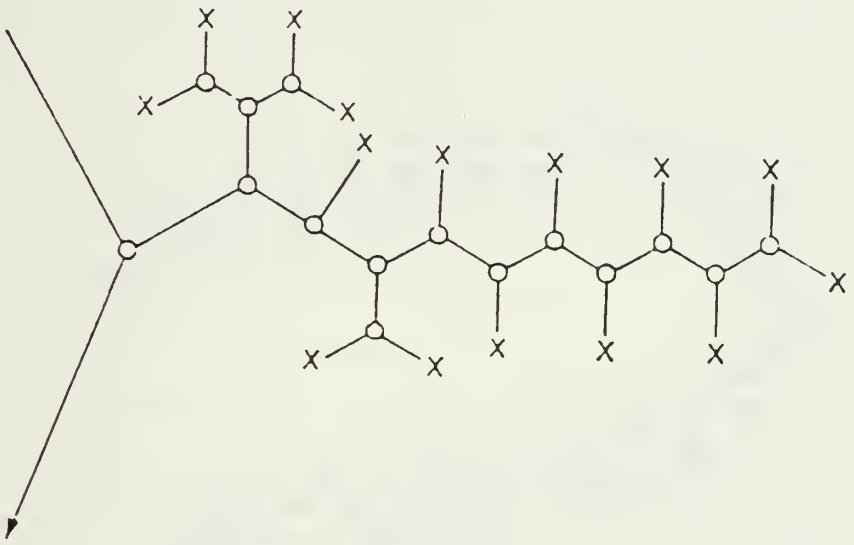

Fig. 1 A spike of displaced atoms (x) and vacancies (o) (Ref. [4])

The displacement spike is the result of the cascade of displaced atoms forming interstitials surrounding a hollow core of vacancies or a depleted zone. A more detailed version of the basic displacemnt spike is shown in Figure 2. Both Figure 1 and Figure 2 represent simplistic models of a displacement spike. Examining these figures it would seem obvious that the configuration would be unstable and that many of the interstitials and vacancies would combine, although certainly not all of them. Seeger, [6], improved on Brinkmans model of the displacement spike by accounting for the effect of focussed collision sequences where atoms

struck by the PKA travel longer distances. Seeger's version of a displacemnt spike is shown in Figure 3.

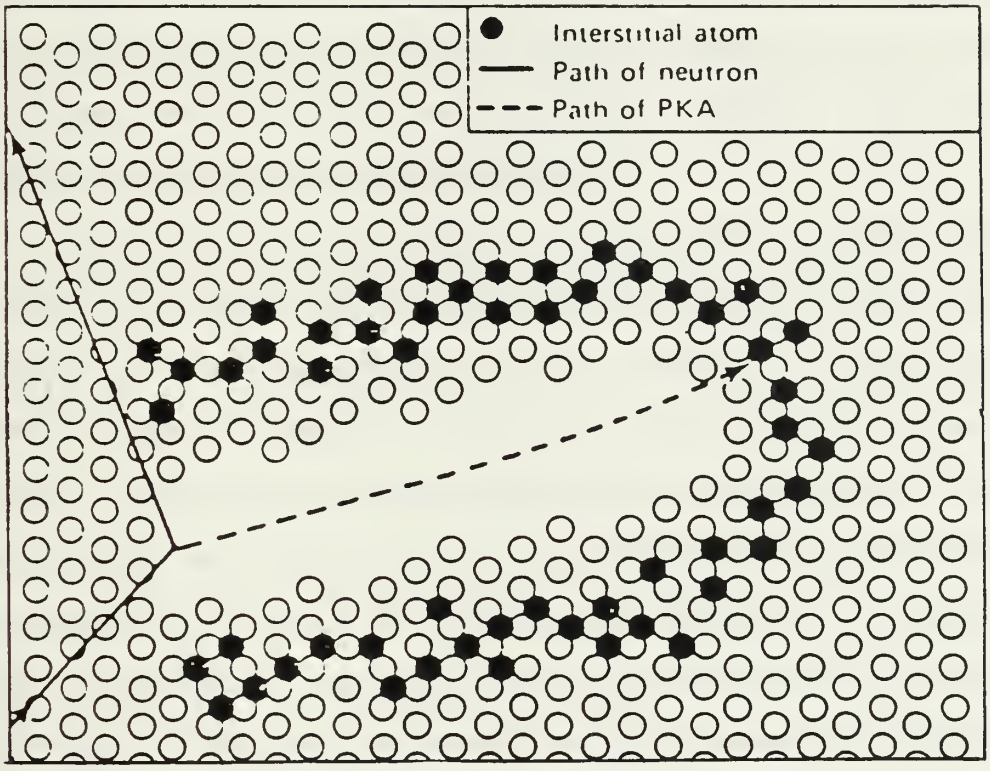

Fig. 2 Original version of a displacement spike (Ref. [2])

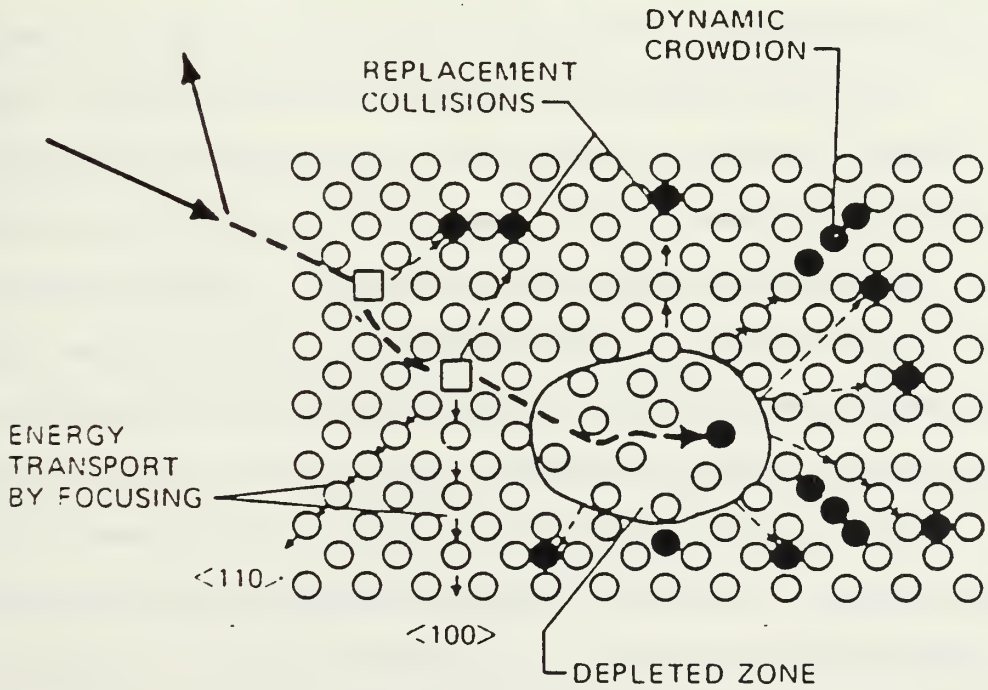

Fig. 3 Later version of a displacement spike (Ref. [2])

In Figure 3 we again have a shell of interstitial atoms surrounding an area of vacancies, but in this model the interstitials are further displaced from the vacancies, and, accounting for recombinations of Frenkel pairs, there are fewer interstitials and vacancies. Seeger called the area of vacancies the depleted zone.

Focussing is a process by which struck atoms travel greater distances than basic collision cascade theory would predict. Focussing refers to the transfer of energy to atoms by nearly head-on collisions along a lattice row of atoms. Channeling is the complementary process to focussing where atoms are able to move long distances in the solid along open directions in the crystal lattice. In looking at these processes it is easy to see why channeled or focussed atoms would make up a disproportionate amount of the final interstitials of a collision cascade. Atoms moving along a crystallographic direction favorable to channeling will lose their energy only by glancing collisions with the surrounding atoms along the channel. Many of these glancing collisions will result in an energy transfer which is less than E_d. This results in more energy being lost by the channeled atom in subthreshold collisions than would be predicted by the cascade theory. Also, these atoms will be able to travel much longer distances before dissipating their energies and settling into interstitial sites. Because of the greater distances traveled, focussed atoms represent a large percentage of the interstitials that escape recombination with the vacancies of the cascade.

Figure 4 shows the basic concept of the focussed collision.

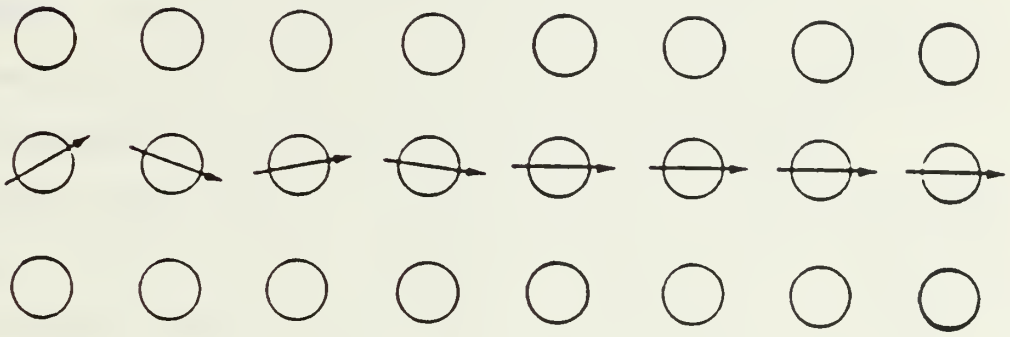

Fig. 4 Sequence of focussed collisions (Ref. [4])

The neutron that initiated the first PKA will then continue to interact with other lattice atoms, initiating additional PKAs until its energy is below the threshold required to displace atoms.

These interacting fast neutrons will generate various types of simple defects. These include point defects, impurity atoms (atomically dispersed transmutation products), small vacancy clusters (depleted zones), dislocation loops (vacancy or interstitial type), dislocation lines (loops that have joined the dislocation network of the original microstructure), cavities (voids), and precipitates. The simple point defects, or Frenkel pairs, are the simplest radiation defects. A crowdion is an interstitial atom in the atomic lattice that forms a close packed line with the original lattice atoms. When a

collision cascade is produced in a metal at a temperature greater than absolute zero, thermal motion of the point defects will produce recombinations and clustering. Clustering, the process where point defects cluster together, is produced when the interstitials or vacancies diffuse into each other. Continued motion or diffusion is then blocked by the presence of the other defects. Orlander, [2], reports that only about 7% of the vacancies present in the cascade, whether clustered or not, survive the initial annealing period as monovacancies. The rest, about 13% of the original quantity, are contained in clusters of four or more vacancies. This initial annealing period during which the spike matures into a more or less stable entity requires from 10^{-7} to 10^{-6} seconds. Naturally, the higher the temperature the irradiated metal is at, the faster and more complete will be this annealing effect. What remains after the initial collision cascade and subsequent annealing period is a collection of practically immobile clusters of interstitial atoms and vacancies and a few sluggish monovacanies. The clusters may either very slowly atrophy by thermally shedding point defects or grow by accretion of mobile point defects from the environmnet or other nearby cascades, [2]. Line defects are defects where a loop is formed by a series of point defects. The line defect then moves through the lattice as a single larger defect.

A schematic representation of the successive steps leading to measurable damage in solids due to fast neutrons

is given in Figure 5. All theories of radiation damage follow this basic block diagram. The more advanced and technical theories just include more variables along the path to account for realistic and actual conditions.

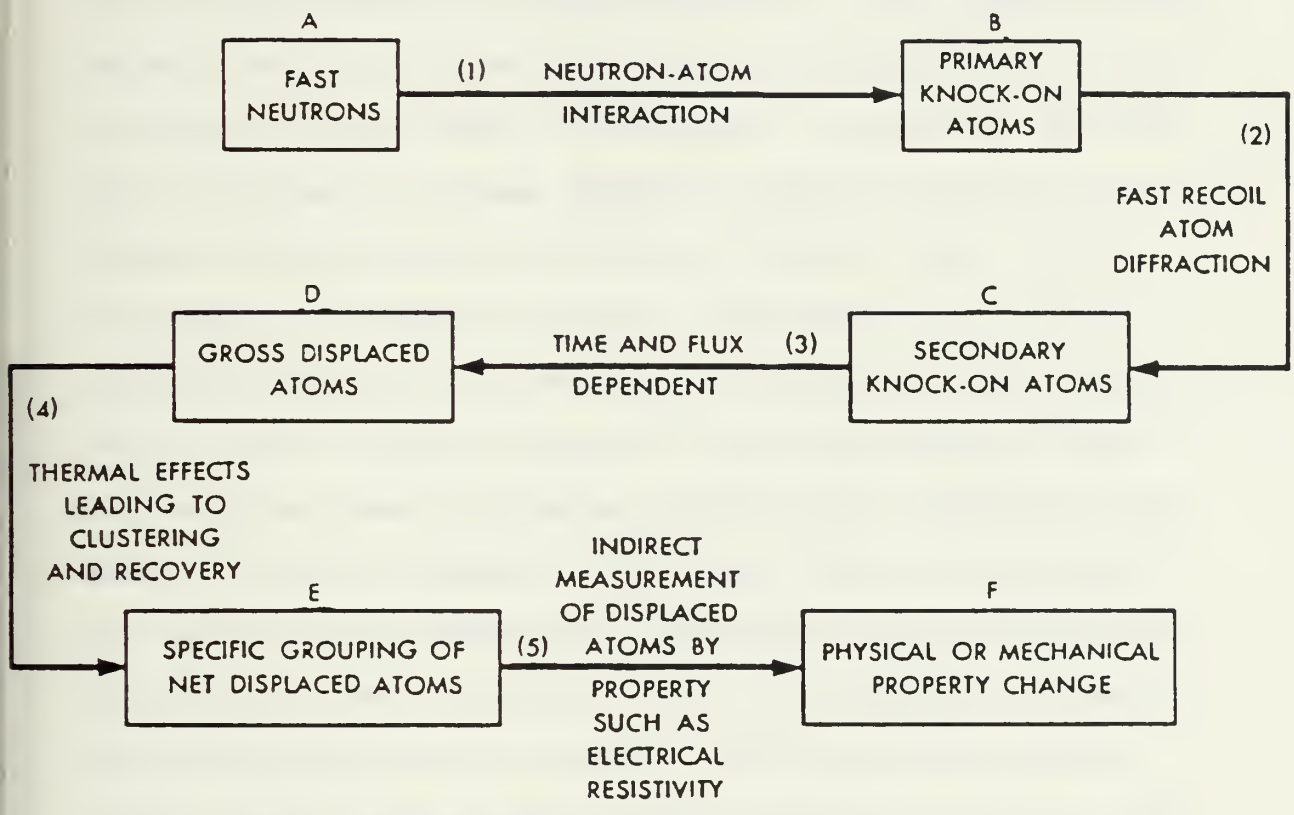

Fig. 5 Schematic diagram of the damage mechanism in a neutron-irradiated solid (Ref.[8])

All defects have the ability to move through the material. In order to move, energy is required to overcome the binding energies holding the defect in place. This energy can be applied thermally or by outside forces or stresses. A piece of steel at normal room temperature has more than sufficient thermal energy to move defects.

Theoretically, thermal atomic motion is possible at all temperatures above absolute zero. Additionally, a normal piece of metal also has numerous physical stresses on it that can move these defects or dislocations. Manufacturing stresses or mechanical stresses applied during construction also provide energies to move defects. Thus, after forming, defects may move around until they reach a barrier or sink of some kind that stops its movement. Typically, the sink that stops or pins these defects, whether interstitial or vacancy, are clusters of defects, depleted zones, grain boundaries, or impurity atoms in the base metal lattice. Bush, [8], points out that impurity atoms in alloys play a major role in cluster formation, and such effects should increase the level of damage assumed from a depleted zone model. Diehl and Seidel, [9], report that in bcc metals, the influence of interstitial additions on the irradiation hardening is very pronounced even if the concentrations of these additions are very small. Thus, an alloy such as HY-80 steel that has many alloying atoms in its basic iron matrix has the potential of pinning many radiation defects and of providing numerous sites for clustering. Of course, it is these same alloying impurity atoms that were purposely added to the iron in order to enhance or change some of its mechanical or physical properties so as to provide a material most suited for its intended purpose.

Alloying elements are generally added to increase the strength and hardness of a material. This is accomplished through the distortion of the lattice structure caused by

the alloyed atoms. The lattice distortion creates a strain along slip planes and grains of the material, which result in the increase of strength and hardness.

HY-80 steel is classified as a Nickel-Chromium-Molybdenum steel although it also has other alloying elements in it. Neely, [10], states that chromium is generally added to improve corrosion resistance, nickel is added to increase ductility and corrosion resistance, and molybdenum is used to promote deep hardening and to increase tensile strength and hardness.

When discussing radiation damage one must also include comments on recovery. Recovery is the annihilation of the Frenkel pairs due to recombination or replacement collisions. As mentioned earlier, a high percentage of defects recover almost immediately. This is especially valid for those materials at the usually high reactor operating temperatures. A small percentage will be trapped in sinks such as impurity atoms, clusters, dislocations loops, or grain boundaries. Cottrell, [4], states that in alloys the recovery from radiation damage tends to be spread out to somewhat higher temperatures because the point defects get trapped at foreign atoms. The number of defects retained will be a function of metal purity, crystal structure, and specimen temperature. The retained defects will be more stable and therefore tend to have a greater effect on mechanical properties.

III. THE EFFECTS ON MECHANICAL PROPERTIES

The major mechanical properties that are affected by neutron irradiation are tensile strength, hardness, impact resistance, creep resistance, stress-rupture failure, and fatigue. This section discusses the tests performed on a material to measure the first three of these properties - tensile, hardness, and impact. These tests include the tensile test, the Charpy V-notch test, and the Rockwell hardness test. The properties measured by these tests include yield strength, ultimate temsile strength, hardness, and impact toughness. Additionally, the method ued to determine the ductile-to-brittle transition temperature from the Charpy impact test is discussed. Finally, the methods by which materials deform are covered, as well as how this deformation is affected by radiation defects.

The strength of a metal is its ability to resist changing its shape or size when external forces are applied to it. There are three basic types of stresses: tensile, compressive, and shear. The strength of materials is expressed in terms of pounds per square inch (psi). This is called unit stress which is equal to the load divided by the total cross sectional area to which the load is being applied. When stress is applied to a metal, the metal changes shape. For example, a metal in tension will stretch longer, and one in compression will shorten. The change in shape is called strain and is expressed in terms of inches of deformation per inch of material length.

The tensile test of a material is performed on a tensile tester which is a machine that applies a tensile (or pulling) load to a standardized specimen. The tester, as it applies the load, also charts the load versus the strain until the sample breaks. Figure 6a shows three representative stress-strain curves; one for a high carbon steel, one for a structural steel, and one for pure iron. Fig. 6b shows a typical stress-strain curve for a general ferritic steel.

The center curve of Figure 6a is for a structural steel and is similar to what should be seen for a high strength steel such as HY-80. As can be seen in the figure, several mechanical property characteristics can be determined. These are:

a = the elastic limit, also called the proportional limit. It is the greatest load a material can withstand and still spring back to its original shape when the load is removed.

b = the yield point, also called the yield strength. It is a point slightly higher than the elastic limit. For most cases, they can be considered the same. The allowable safe load for a metal in service should be well below the elastic limit or the yield point.

c = the ultimate strength, also called the ultimate tensile strength. It is the highest strength that a metal exhibits after it begins to deform plastically under load.

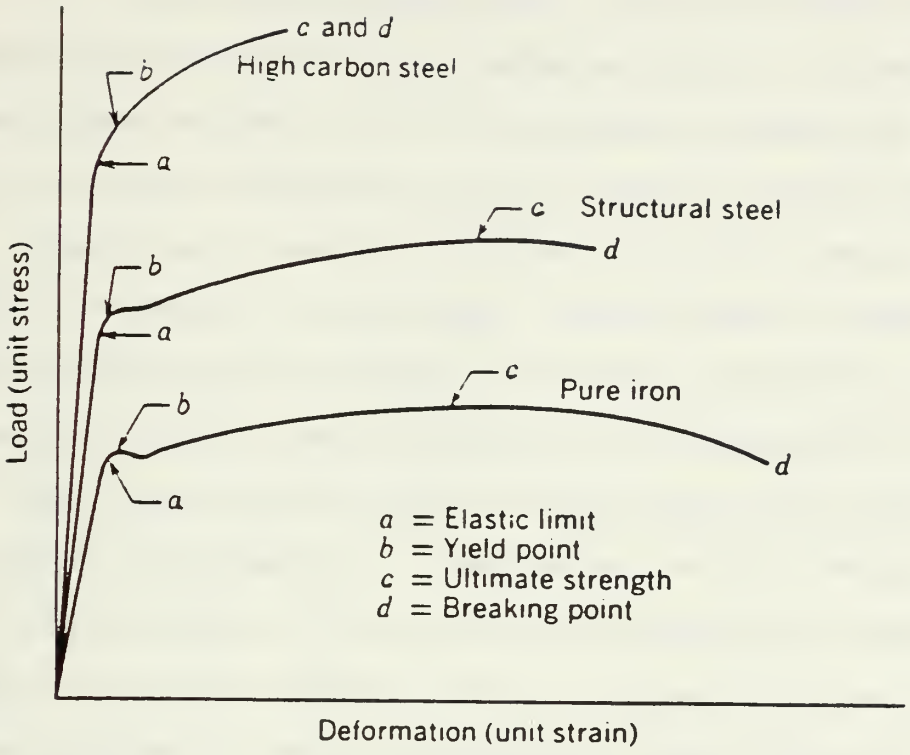

(6a) Stress-strain diagrams (Ref. [10])

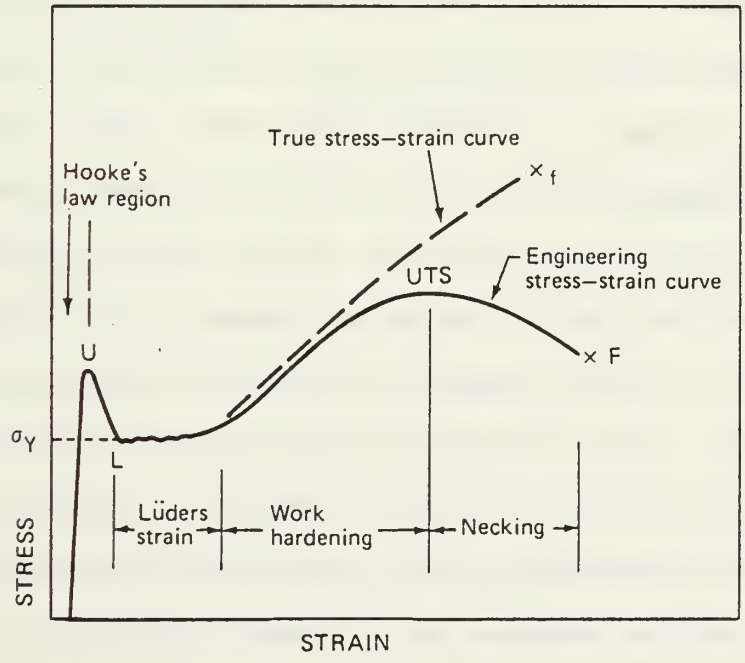

(6b) Stress-strain curve for a ferritic steel (Ref.[2])

Fig. 6 Representative Stress-strain curves (Ref. [2,10])

d = the breaking point. It is the point or strength where rupture of the material occurs. It usually occurs either at the peak of its ultimate strength or at a point of further elongation and at a drop in stress load.

Figure 6b is similar to Figure 6a, but it shows a little more detail in the curve. Notice that it shows an upper yield point, U, as well as a lower yield point, L. The point U is the same as the point b as depicted in Figure 6a. After the initial yield, the load drops with increasing elongation to the point L. The reason for this sharp yield point is attributed to the pinning of dislocation lines by impurity atom (principally carbon) strings along the line. For deformation to occur, dislocation lines must move through the medium along its slip planes. Stress fields around dislocation lines can attract impurity atoms. These atoms, in turn, act to pin the dislocation and prevent it from moving. Thus, additional stress is required to start the dislocation moving. Once free from the pinning action of the impurity solute atoms, the dislocation can move at a lower stress, which causes the drop in the yield stress from U to L. For a short interval following point L, plastic deformation proceeds with no increase in load. This interval is called the Luders strain. Following the Luders strain is the work-hardening or strain-hardening region. In this region the stress required to produce further strain increases because the material becomes stronger as a result of the deformation process.

The elastic range and plastic range of a metal can also be seen on the stress-strain diagram. Figure 7 shows an example of this.

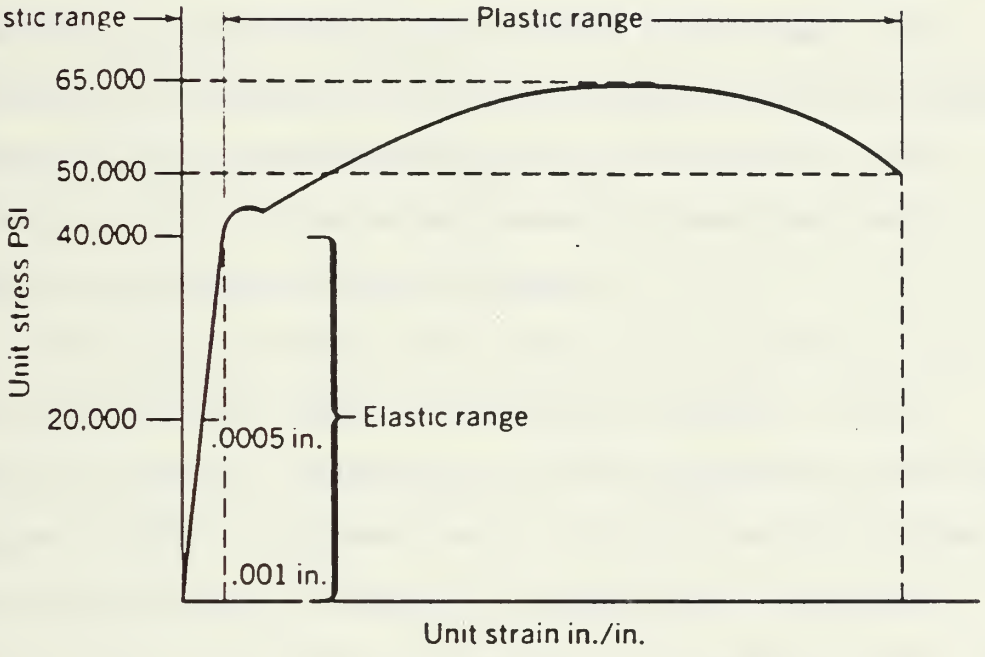

Fig. 7 Stress-strain diagram for a ductile steel (Ref.[10])

For the steel in question, HY-80 steel, the minimum yield strength is 80,000 psi. In other words, the yield strength for the specimens of HY-80 steel that are to be tested should not be less than 80,000 psi.

Hardness is the property of a metal that measures its ability to resist being permanently deformed by penetration. The amount of penetration decreases as the hardness of the specimen increases. Generally, the harder the material, the greater is its tensile strength. Thus, we would expect to

see the same trends, after irradiation, in hardness as we would see in tensile strength. Rockwell and Brinell hardness testers are the most commonly used types of hardness testers for industrial and metallurgical purposes.

The Rockwell hardness test is made by applying two loads to a specimen and measuring the difference in depth of penetration between the minor and the major load. The difference is measured on arbitrary scales that are accepted worldwide and called Rockwell A, B, or C scales. The Rockwell C scale is the scale generally used for hard materials such as structural steels.

The impact property of a metal is a measure of its ability to resist rupture from impact loading. It is generally known as toughness or notch-toughness of the metal because the test specimens have a pre-cut notch in them. The standard testing machine is called the Izod-Charpy machine and it consists of a weight on a swinging arm. The arm or pendulum is released, strikes the specimen, and continues to swing forward. The amount of energy absorbed by the breaking specimen is measured by how far the pendulum continues to swing. A brittle material is one that absorbs very little energy before breaking while a tough material would require a large expenditure of energy to break it. Hertzberg, [11], points out that for an unnotched tensile bar, the energy to break the specimen may be estimated from the area under the stress-strain curve. The basic formula for this is represented as follows:

$$\text{energy} = \int_0^{\epsilon_{final}} \sigma \, d\epsilon$$

where σ = strain

ϵ = stress

Thus, by measuring the toughness, we obtain another piece of information about a material's mechanical properties. Figure 8 shows three stress-strain curves with their representative toughness indicated by the shaded areas under the curves.

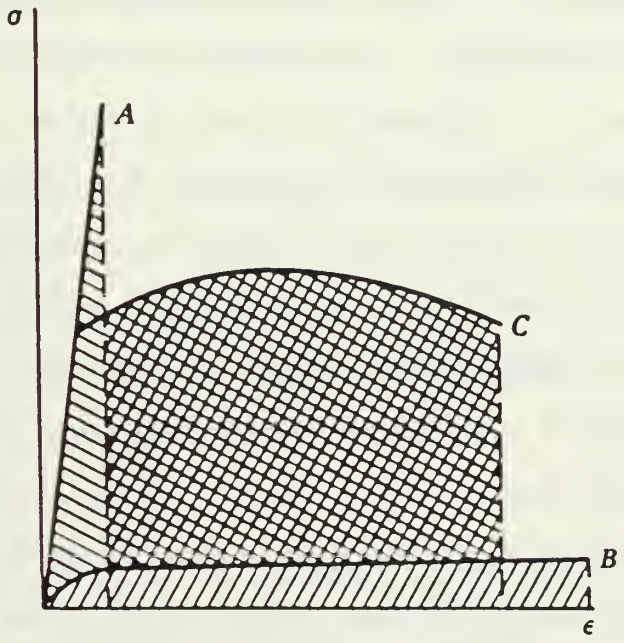

Fig. 8 Stress-strain curves showing toughness (Ref. [11])

Curve A in Figure 8 represents a strong material with little plastic deformation. Curve B represents a low strength but highly ductile material. Curve C represents a material with an optimum combination of strength and ductility for maximum toughness. Curve C is similar to what would be seen in a high strength structural steel such as HY-80.

Brittleness is a term to describe the property of a material that fails with little or no plastic deformation. It is the property opposite to plasticity. Cottrell, [4], reports that except for face-centered-cubic (fcc) metals, virtually all solids become brittle at low temperatures.

The transition from ductile behavior to brittle behavior generally occurs in a narrow range of temperature so that it is possible to characterize a material by a certain transition temperature. Below the temperature the material exhibits brittle behavior, and above the temperature it exhibits ductile behavior. This temperature is called the ductile-to-brittle transition temperature (DBTT) and generally it is in the range of -50 to +20 degress Celsius for unirradiated mild steels, [2]. In the tensile test, brittleness can be correlated to the reduction in area of the specimen before breaking. A brittle specimen would have little or no reduction in area prior to breaking, while a ductile specimen would have considerable reduction in area. In the Charpy impact test brittleness can be correlated to the amount of energy absorbed prior to fracture. As stated before, a brittle material is one that

absorbs very little energy prior to rupture. Consequently, the Charpy impact test can be used to determine the ductile-to-brittle transition temperature of a metal. By conducting the impact test at a wide range of temperatures, a graph of energy absorbed versus temperature is developed. Figure 9 shows a sample transition temperature curve for a steel. It also shows a curve relating the reduction in area during a tensile test conducted at different temperatures. The transition temperature for this example would be about 320°K. This corresponds to an energy absorbed of about 30 FT.LBS. or 40.7 Joules, which is arbitrarily used to separate ductile and brittle regimes,[2]. The nil-ductility-temperature (NDT), below which the metal appears brittle even in plain tensile tests and the reduction in area drops sharply to almost zero, correlates well with the DBTT, and the two terms are used interchangeably.

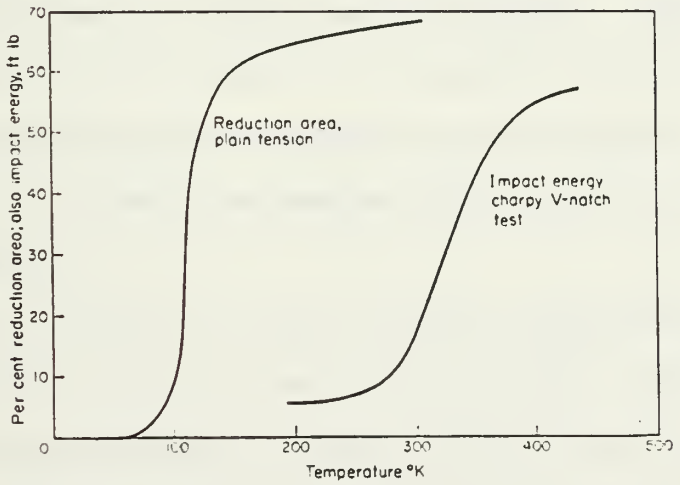

Fig. 9 Ductile-brittle transition (Ref. [4])

Even prior to irradiation, metals are marred by a variety of defects that are produced during formation of the grains from the original melt or by working or deforming the material. These include point defects, dislocations, and grain boundaries.

The point defect is an imperfection associated with one or perhaps two lattice sites. Point defects include vacancies, interstitial atoms, and impurity atoms. The vacancy and the interstitial are intrinsic point defects since they do not depend upon the presence of a foreign substance as does an impurity. Thermodynamically, a perfect crystal is possible only at 0°K; therefore, vacancies and interstitials must exist in any crystal. Impurity atoms in a crystal lattice behave much as do interstitials and vacancies. Some impurities are a result of the normal manufacturing process where it is nearly impossible to keep all unwanted impurities out, but many impurity atoms are purposely added as alloys in order to enhance the base crystals physical or mechanical properties. Point defects are of concern to the study of irradiation effects because their presence controls the mobility of atoms in a solid which in turn affects the mechanical properties and response of the material.

A grain boundary is the surface separating different grains. Grains are the individual crystals that are formed during the solidification of the liquid in the manufacturing process. Under ordinary manufacturing conditions, many nuclei are formed and grow into many adjoining crystals to

make up the polycrystalline structure. These crystals grow until they encounter adjacent crystals at their boundaries. A grain boundary is no more than a few atoms thick - just enough to adjust for the misorientation of the lattice structures of the neighboring grains. Figure 10 shows a simple diagram depicting a polycrystalline substance. The solid continuous line between the crystals in Fig. 10b are the grain boundaries.

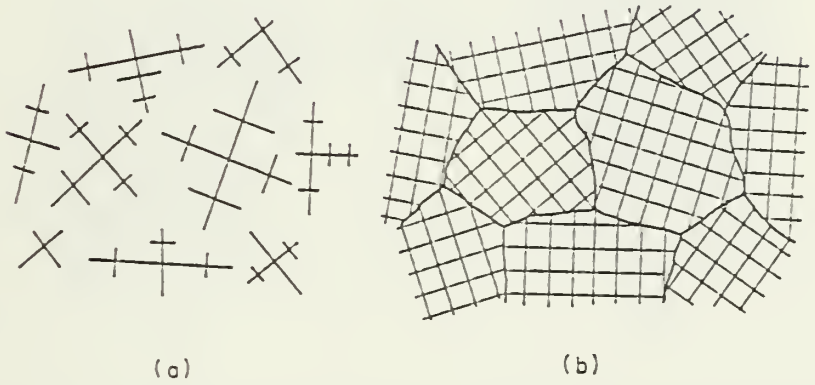

Fig. 10 Formation of dendrites (a) leading to a polycrystalline structure (b) (Ref. [4])

Figure 11 shows a close up view of the two general types of grain boundaries between like crystals. Small-angle boundaries, Fig. 11b, are tilted only a few degrees and are composed of a nearly parallel stack of edge dislocations. Large-angle grain boundaries, Fig. 11a, are tilted by angles of misorientation greater than 20 degrees. Large-angle grain boundaries provide larger gaps in the

crystal lattice to which interstitials and impurities can collect. Grain boundaries not only can collect other defects that can affect the mechanical properties of the material, but their own orientation and surface energies also contribute to the characteristics of the substance.

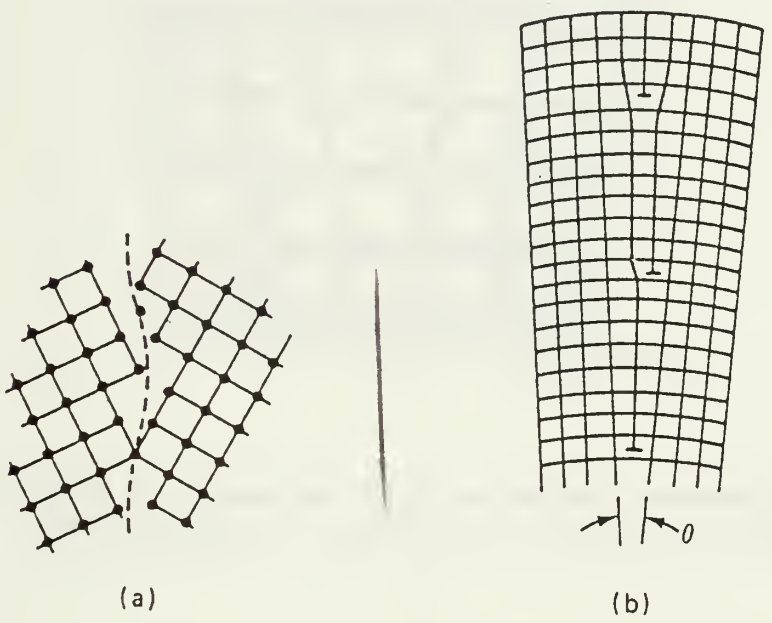

Fig. 11 Grain-boundary models: (a) Large-angle grain boundary (b) Small-angle grain boundary (Ref. [2])

A dislocation is a lattice line defect that defines the boundary between slipped and unslipped portions of a crystal. There are two basic types of dislocation defects. These are the edge dislocation and the screw dislocation.

The edge dislocation is defined by the edge of the extra half plane of atoms as shown in Figure 12, [11]. Note that the extra half plane is wedged into the top half of the crystal. This lattice distortion creates a very high energy

region in the area of the dislocation.

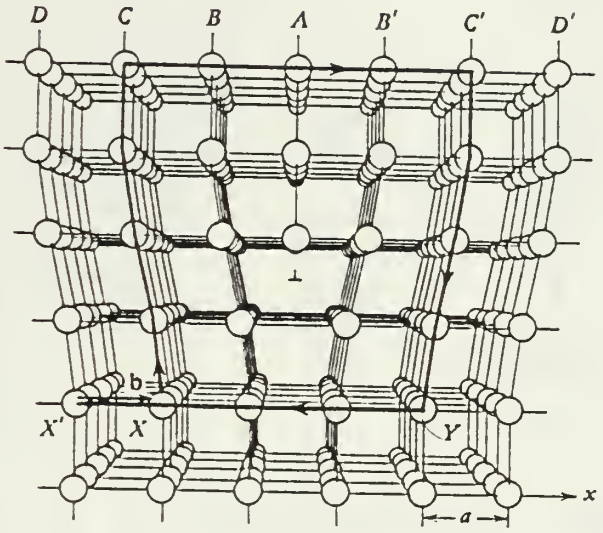

Fig. 12 Edge dislocation lattice defect caused by introduction of extra half plane of atoms (Ref. [11])

The screw dislocation is so named because of the helical pattern, resembling a ramp, which is described by the continued rotation of the dislocation into the crystal. A diagram of a screw dislocation is shown in Figure 13.

Edge and screw dislocation can combine to form what is called a dislocation loop. The dislocation loop does not need to be straight and it need not terminate on an external surface of the crystal. A dislocation loop can reside completely within the crystal, and the loop can move as a single entity through the crystal as do single edge or screw dislocations.

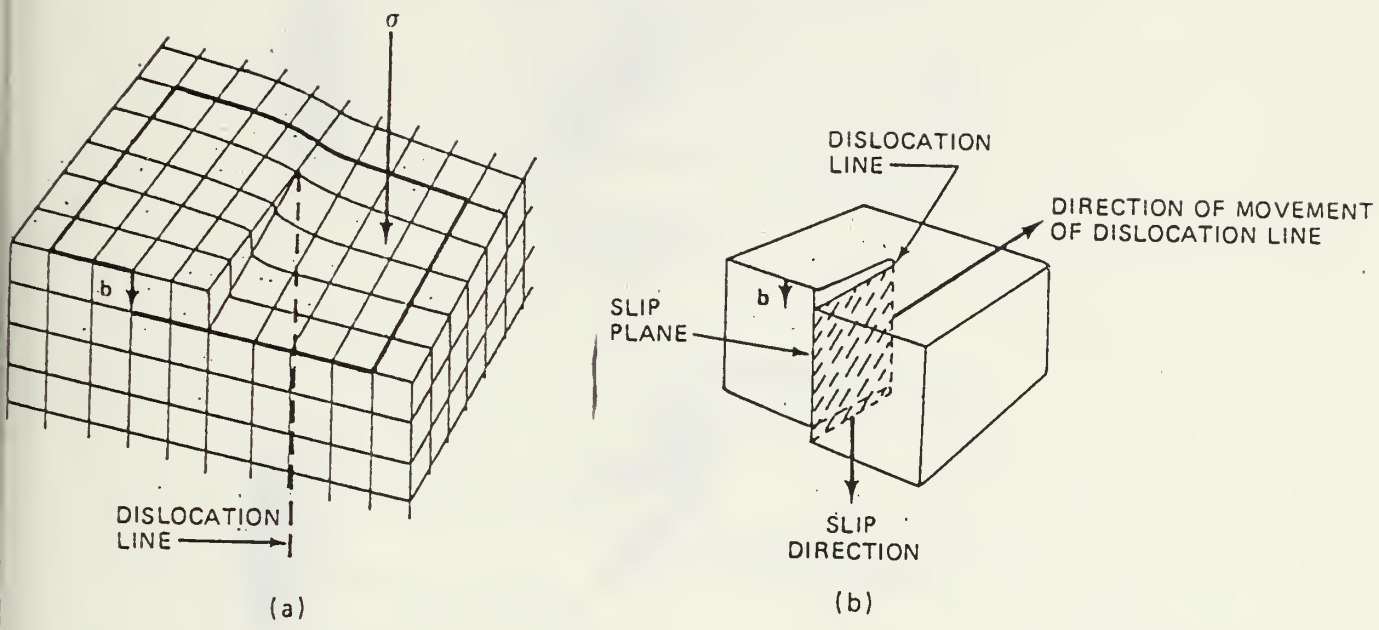

Fig. 13 The screw dislocation (Ref. [2])

Dislocation theory was introduced to explain why it took much lower stress to deform a crystal than theory predicted for that perfect crystal. It is the movement of dislocations in and through various slip planes that leads to deformation. Slip is the movement a crystal makes along a particular crystallographic plane when sufficient force is applied. Figure 14 shows the basic mechanism of how slip leads to plastic deformation. A unilateral tensile force is applied to the crystal resulting in slip and subsequent deformation. In bcc crystals slip occurs in the (110), (112), and (123) planes, [2]. Additionally, slip occurs in the [111] direction for bcc materials. Figure 15 shows a diagram of a bcc crystal with a slip plane designated.

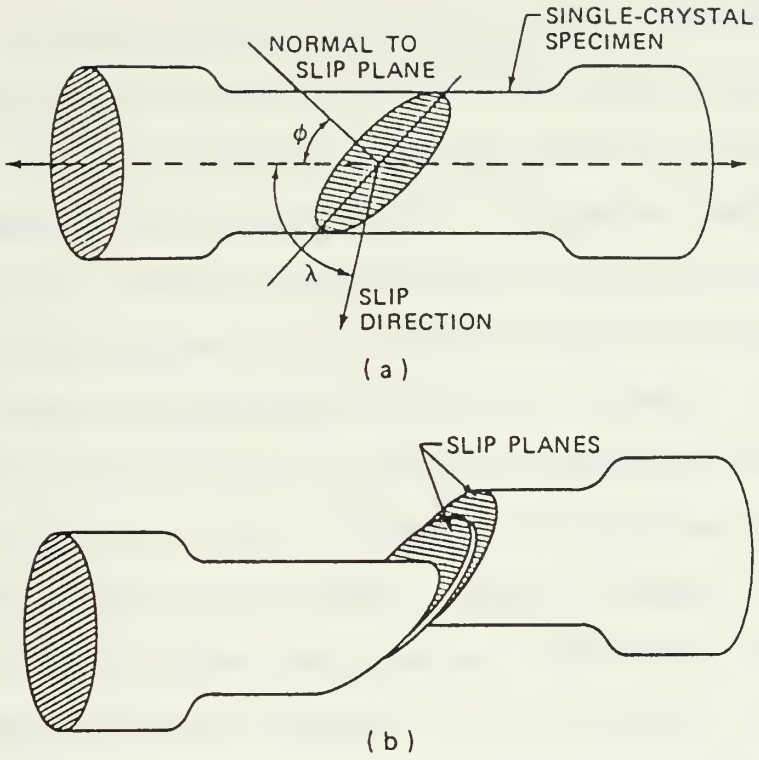

Figure 14 Plastic deformation of a single crystal (Ref.[2])

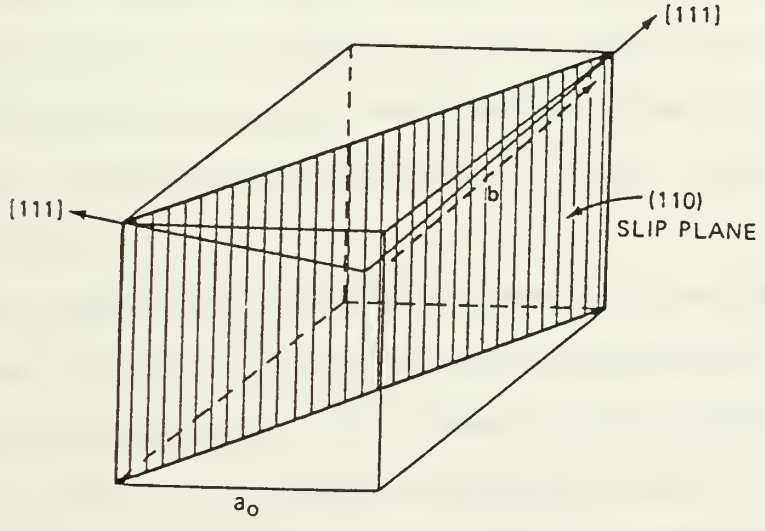

Figure 15 Slip planes and slip direction in bcc crystals (Ref. [2])

It is the movement of dislocations along their slip planes that lead to deformation if sufficient stress is applied. As the dislocations move along their slip planes, their movement can be hindered or stopped by obstacles in the material. These obstacles can be grain boundaries, point defects, other dislocations, clusters of vacancies, precipitates, or alloying interstitial atoms. If plastic deformation is to occur or continue, energy is required to move a dislocation over, around, or through an obstacle that may be blocking its path. Often, thermal energy is sufficient to provide the necessary additional energy to keep the dislocations moving. This is why at higher temperatures one generally finds materials to be more ductile. This additional stress required to keep the dislocation moving is a measure of the increase in strength of a material caused by the presence of the defects. When the material reaches a point where all the dislocations are pinned or clustered together such that they can no longer move, then further plastic deformation is not possible. Breakage of the material will occur if the stresses continue to increase.

As stated earlier, dislocations can overcome some obstacles in their paths by various mechanisms if there is sufficient energy available. Some of the mechanisms employed by the dislocations to overcome barriers include glide, climb, cross-slip, and looping. Detailed explanations of these phenomena can be found in references [4] and [11], or in most metallurgy textbooks.

As discussed above, the presence of obstacles hinders the movement of dislocations, requiring additional energy to maintain plastic deformation. This then results in strengthening or hardening of the material. The presence of radiation defects provide the same results as do natural defects in a material. The radiation defects act as obstacles to dislocation movement; therefore strengthening or hardening the material. The term "radiation hardening" is often used to describe this process. Point defects and impurity atoms are believed to contribute negligibly to hardening compared to the effect of the larger defect clusters, [2]. At the same time, the presence of radiation defects can lead to embrittlement of the material by preventing any plastic deformation prior to failure. The term "radiation embrittlement" is often used when discussing the effects of neutron radiation on various materials.

Generally, researchers have found that neutron irradiation raises the yield strength and the ductile-brittle transition temperature. At the same time, there is a corresponding decrease in tensile ductility and Charpy impact shelf energy, [11]. Figure 16 is a diagram showing irradiation-induced changes in Charpy impact response for a typical reactor-vessel steel. Note, that the higher fluence levels cause greater embrittlement. Although the exact cause of this embrittlement is not clearly understood, it is believed to be related to the interaction of dislocations with defect aggregates, such as solute atom vacancy clusters that are generated by neutron bombardment,

[11]. Studies have also shown that the extent of irradiation damage depends strongly on the irradiation temperature, with more damage accompanying low temperature neutron exposures.

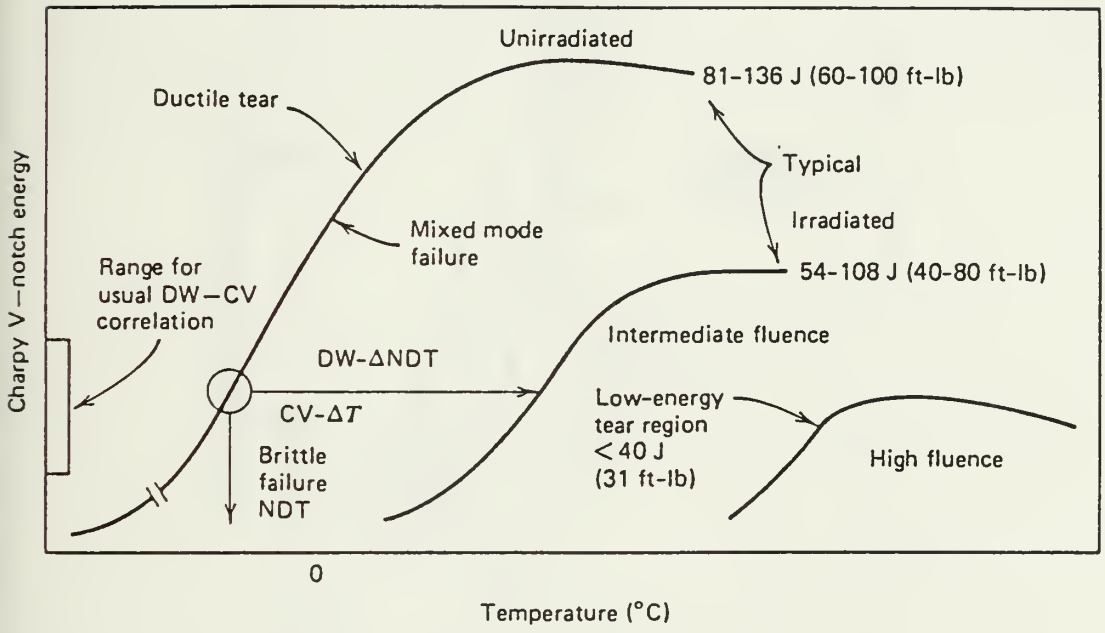

Fig. 16 Transition temperature shift resulting from neutron-irradiation (Ref. [11])

Figure 17 shows a diagram relating the effects of fast neutron fluence on the increase in the nil-ductility-temperature of low carbon steels that were irradiated at various temperatures. Notice that increasing the fluence increases the NDT, and that the irradiation temperature plays a strong role in the extent of the NDT change. The higher the irradiation temperature, the less the increase in

NDT. This is due to the natural annealing of defects that occurs at the higher temperatures.

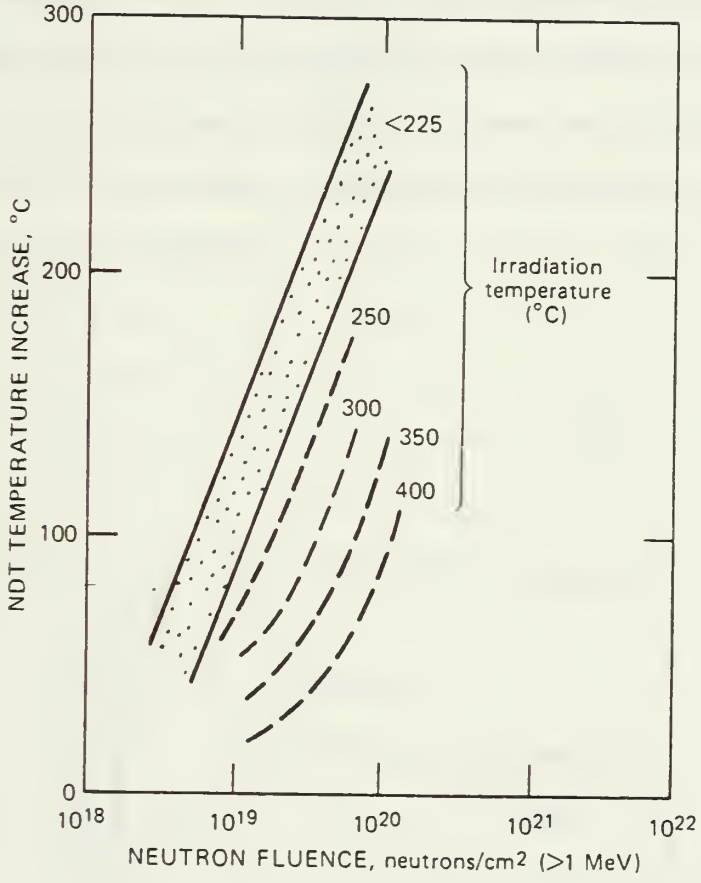

Fig. 17 Effect of fast neutron fluence on the increase in the nil-ductility-temperature (Ref. [2])

Radiation hardening usually means the increase in the yield stress and the ultimate tensile stress as a function of fast neutron fluence. In both austenitic and ferritic steels, irradiation increases the yield strength much more than it does the ultimate tensile strength (UTS). This

approach of the yield strength to the UTS is responsible for the ductility loss that is also found with increasing fluences, [2]. Figure 18 is a diagram showing the effects of fast neutron fluences on the tensile properties of steels. The increasing fluence effects are shown in the upper three curves. Note that the uppermost curve shows a case where the yield strength and the UTS coincide. This specimen would be very brittle. This could also be deduced by the small area under the curve, indicating a material that is not very tough.

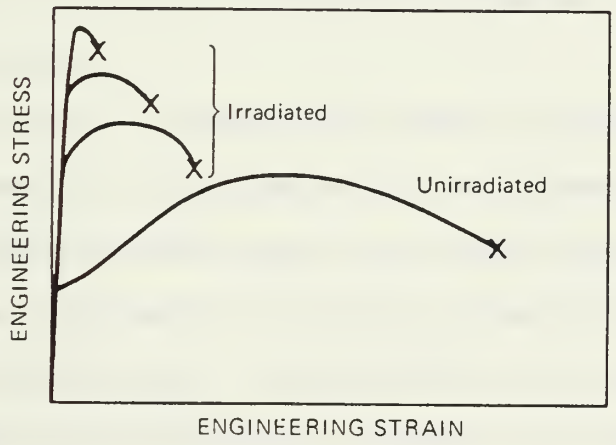

Fig. 18 Effect of fast neutron irradiation on the tensile properties of reactor steels (Ref. [2])

In brief summary, radiation strengthens a metal in two different ways, [2].

1. It can increase the stress required to start a dislocation moving on its glide plane. The resistance to dislocation startup is called source hardening. The applied stress required to release a dislocation into its slip plane is called the unpinning or unlocking stress.

2. Once moving, dislocations can be impeded by natural or radiation produced obstacles close to or lying in the slip plane. This is called friction hardening.

In addition to increasing the yield strength with irradiation, the ductility is also reduced. These radiation effects can be reduced by natural annealing if the irradiation occurs at elevated temperatures, or by forced annealing by raising the irradiated component's temperature to higher levels.

For the case of the HY-80 steel in the hull of a submarine where it is subjected to sea temperatures ranging from about 32°F to 90°F, which are relatively low temperatures, one would not expect a significant amount of annealing to take place. Consequently, the majority of induced radiation defects will remain in the hull throughout the lifetime of the vessel.

IV. PREVIOUS RESEARCH ON HY-80 STEEL

This section discusses previous work done by several different researchers on the irradiation effects of fast neutrons on HY-80 steel. It covers the results of these studies and how mechanical properties changed due to the neutron irradiation.

HY-80 and similar strength Ni-Cr-Mo steels are used by the Navy and industry in applications where a strong, tough material is needed. To date, these steels have not been used for the construction of reactor pressure vessels. Instead, the steels normally used for pressure vessel construction include A302-B, A212-B, A201, SA336, and other steels of similar composition. Because HY-80 steel is not used directly in the construction of reactor components, there has been only limited research done in studying the effects of neutron irradiation on its mechanical properties.

Those steels commonly used in pressure vessel construction have been studied thoroughly concerning the effects of irradiation on their mechanical properties. The Ni-Cr-Mo steels have been studied much less, and available data on them is not as numerous as that on the pressure vessel steels. However, as the nuclear industry looks at the use of more fast reactors and possibly the use of fusion in the future, the need to know more about the higher strength steels and their potential applications is very important.

The Military Specification for HY-80 steel, [12],

lists the chemical composition specifications for HY-80 steel plate as shown in Table 1. For comparison, the composition of a A302-B steel is also listed. As can be seen, HY-80 is considered a Ni-Cr-Mo steel due to the higher levels of those elements in its composition.

Table 1 Composition of HY-80 and A302-B Steel (%)

Element	HY-80	A302-B
Carbon (C)	0.10 - 0.20	0.26
Manganese (Mn)	0.10 - 0.45	0.76
Phosphorus (P)	0.020	0.011
Sulfur (S)	0.002 - 0.020	0.031
Silicon (Si)	0.12 - 0.38	0.24
Nickel (Ni)	2.45 - 3.32	0.22
Chromium (Cr)	1.29 - 1.86	0.20
Molybdenum (MO)	0.27 - 0.63	0.02
Iron (Fe)	Remaining	Remaining

The emphasis of radiation-effect studies on steels has been placed primarily on the determination of changes in notch-ductility. The largest impact here is the shift that the change in the notch-ductility has on the ductile-brittle transition temperature (DBTT). For steels irradiated at less than 450°F, a relatively consistent increase in nil-ductility temperature (NDT) is observed with increasing neutron exposures in the range 2 X 10^{18} to 3 X 10^{19} n/cm2

(> 1 Mev). Steels that are irradiated at 510° and 550°F show an increase in NDT which is 75° to 100° less than the NDT increases for the lower temperature irradiations, [13].

Figure 19, from Ref. [13], shows the relationship of the initial NDT values for various steels to normal reactor startup and operating temperatures. It can be seen that HY-80 steel has a considerably lower NDT than the steels used in pressure vessel construction. It can also be seen that because of the low NDT values for HY-80, its application for use in ships' hulls is ideal because sea water temperatures will seldom be below about 32°F. After irradiation, however, if the amount of fast neutron fluences is high enough to shift the DBTT to a point approaching or beyond the freezing point of water, then there would be valid reasons for concern for the integrity of the hull and the safety of the boat. It can also be noted in Figure 19 that the steels presently used in pressure vessel construction would not be suitable for use in constructing ships' hulls.

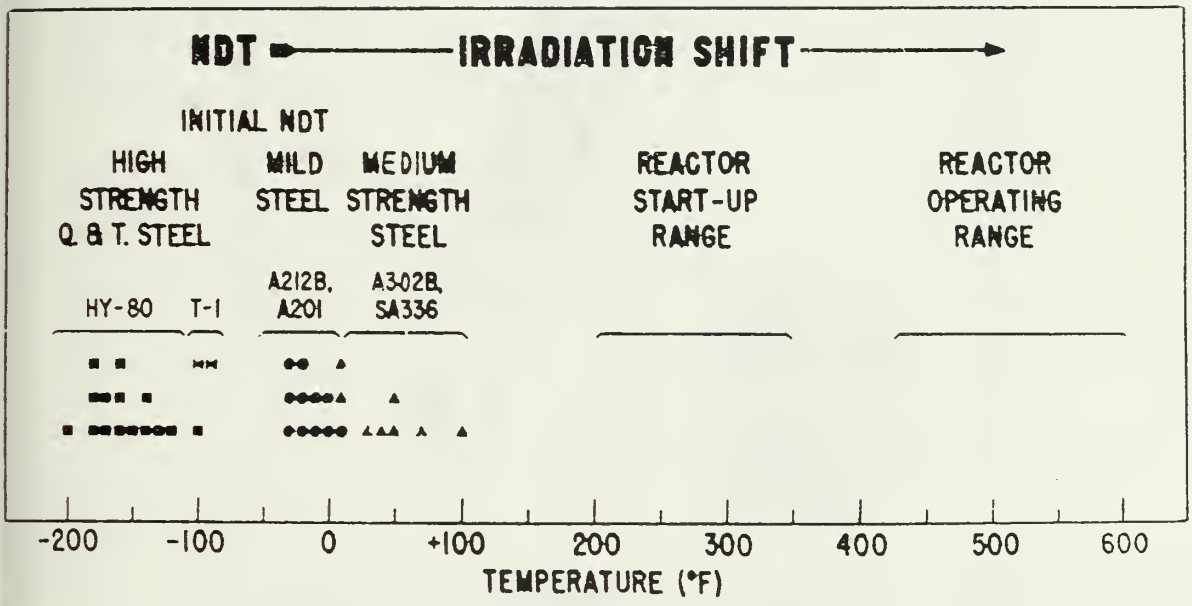

Fig. 19 Relationship of initial NDT of various steels to reactor startup and operating temperatures (Ref. [13])

The U. S. Navy Research Laboratory (NRL) in Washington, D. C. has carried out extensive tests on the irradiation effects on the steels used in pressure vessel construction. Included in these tests have been samples of HY-80 steel for comparison purposes and to see any applicability of HY-80 for pressure vessel use. Figure 20 is a graph showing the increase in the NDT temperature as a result of irradiation below 450°F for several steels, including HY-80, from testing conducted at NRL.

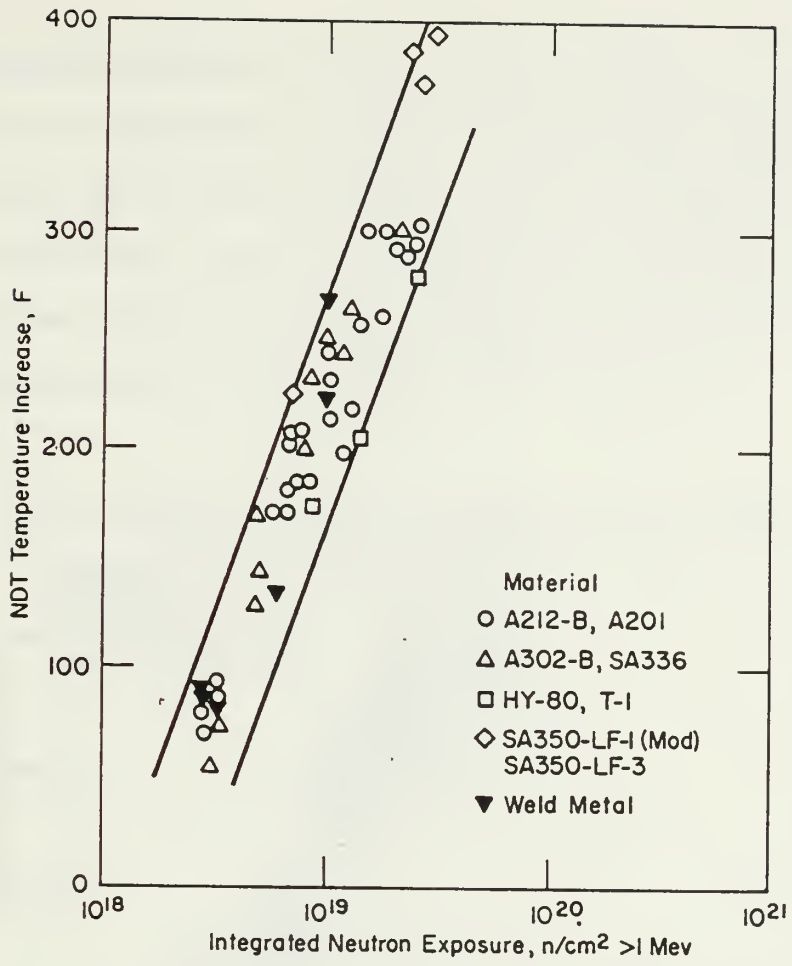

Fig. 20 Increase in the NDT resulting from irradiation below 450°F (Ref. [3])

It can be noted that for the same fluence the HY-80's shift in NDT is less than that for the other steels shown. This would indicate that HY-80 is less sensitive to the irradiation effects than the other steels. It can also be noted that detectable shifts in the NDT do not appear to occur until total neutron fluence reaches a level of around 3×10^{18} n/cm². The 450°F figure is significant because at temperatures less than this no appreciable lessening of radiation effects seems to occur, [3]. This means that

recovery due to either self or induced annealing does not occur to any measurable amount at these lower temperatures.

A more generalized graph, showing a larger collection of data from other sources, is depicted in Figure 21. This graph of the increase in DBTT versus neutron exposure supports the conclusions drawn from Figure 20.

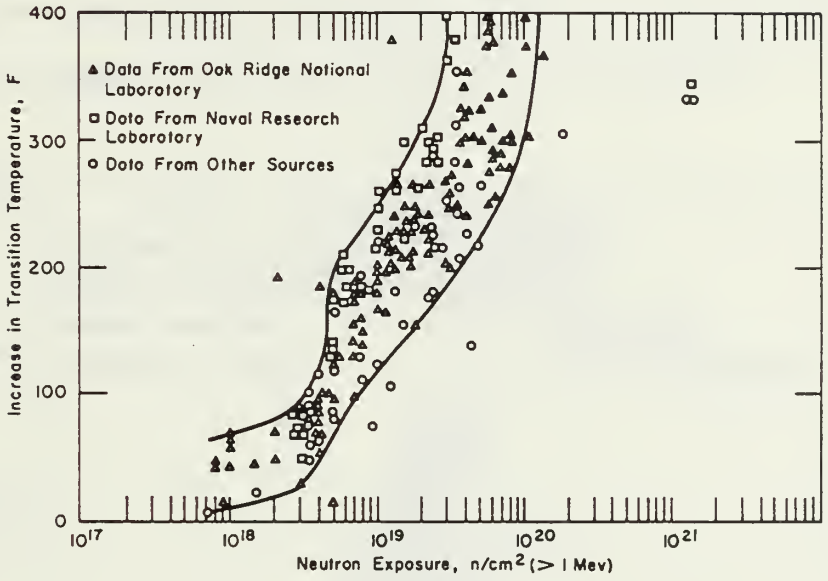

Fig. 21 Effect of neutron radiation on the notch-toughness of carbon and alloy steels irradiated below 500°F (Ref. [3])

As seen in Figure 21, the shift in DBTT does not appear to occur until fluences approach levels around 1×10^{18} n/cm². It can also be seen that the change in DBTT seems to reach a maximum between 1×10^{18} and 1×10^{19} n/cm². This, perhaps, indicates that a saturation level of radiation defects is reached near this level, and that further irradiation does not produce additional changes in the mechanical properties.

When considering a steel for use in the pressure vessel for a reactor one must consider that the reactor operating temperatures are normally in the range of 450° - 550°F. Steele and Hawthorne of NRL irradiated A302-B and HY-80 at 540°, 640°, and 740°F to an integrated flux of 3 X 10^{19} n/cm^2, [14]. The results for the A302-B steel may be noted from the triangle points in Figure 22, which also shows the results of some other pressure vessel steels. Figure 23 shows the results for the HY-80 steel.

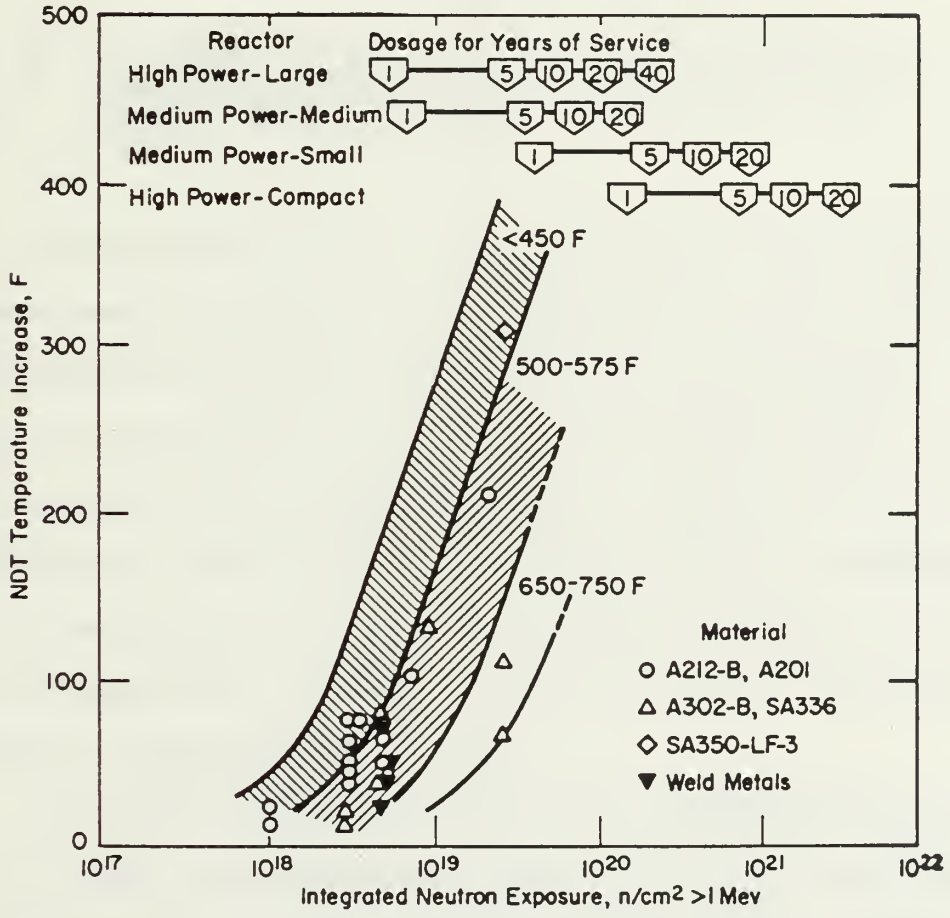

Fig. 22 Increase in the NDT resulting from irradiation at higher temperatures (Ref. [3])

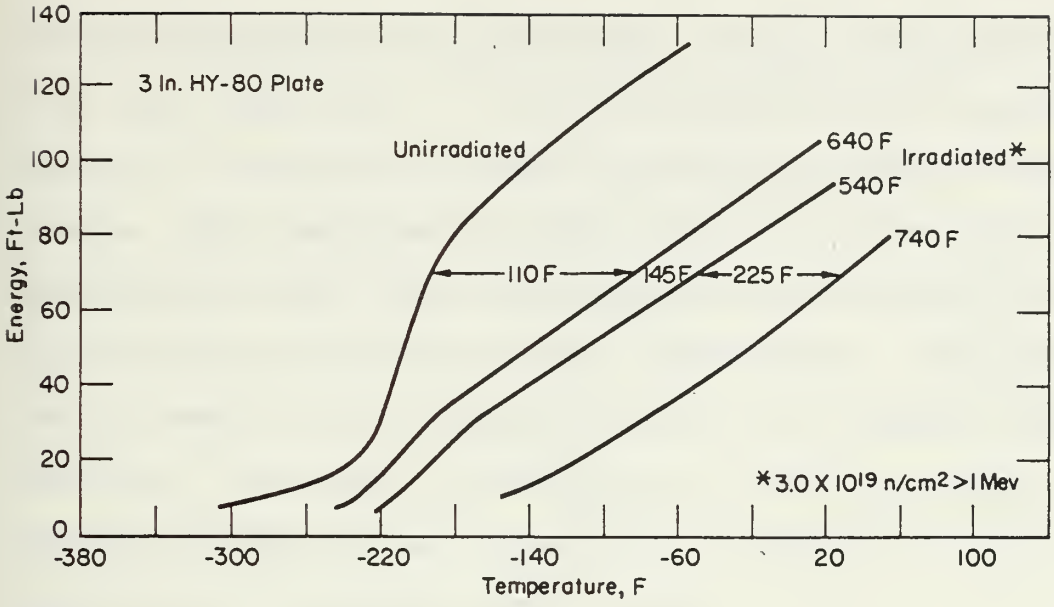

Fig. 23 Transition temperature shifts resulting from elevated temperature irradiation of HY-80 steel (Ref. [3,14])

From Figures 22 and 23 it can be seen that the two steels behaved similarly at 540° and 640°, but at 740° the HY-80 steel had a much greater shift in the transition temperature than had occurred at lower temperatures, and greater than that of the A302-B steel. Subsequent heat treatment of the HY-80 steel at the irradiation temperature for an equivalent period of 2,000 hours, showed that thermal embrittlement alone would not account for the increased transition temperature, [3,14].

In another annealing experiment with A302-B and HY-80 steel, Steele and Hawthorne found significantly different recovery aspects of the two steels. Annealing at 800°F gave about 63% recovery of the transition temperature shift for A302-B irradiated at 640°, but no recovery in HY-80

irradiated at the same temperature. Table 2 lists the data from their experiment. It can be noted that the transition shifts on irradiation at 640°F had been the same for both steels. The researchers suspect that the presence of nickel and chromium affect the annealing behavior of the HY-80 steel after irradiation at high temperatures. Additional testing needs to be conducted to confirm or dispute these theories. Obviously, the ability of a metal to recover from radiation damage through annealing is a property that is desirable in a pressure vessel steel.

Table 2 Comparison of recovery characteristics of HY-80 and A302-B steels irradiated at 540° and 640°F (Ref. [2,14])

As irradiated ΔT °F		Postirradiation anneal	Recovery °F		Recovery %		ΔT after anneal	
Y-80	A302B		HY-80	A302B	HY-80	A302B	HY-80	A302B
145	165	750 F, 24 hr	50	80	34.5	48.5	95	85
		750 F, 72 hr	80	100	55.0	60.5	65	65
		800 F, 24 hr*	70	100	48.5	60.5	75	65
110	110	800 F, 24 hr	0	70	0	63.5	110	40

*Exploratory spot check with limited specimens.

NRL researchers, as reported in NRL Memorandum Report 1808, [15], found the changes in the DBTT for HY-80 steel for several fluence levels at less than 450°F to be as shown in Table 3. Representative values for A302-B steel are also shown.

Table 3 Ductile-brittle transition temperatures for HY-80 and A302-B steel as determined by Charpy V (30 Ft.Lb.) (Ref. [14])

Neutron fluence (10^{19} n/cm^2)	HY-80 DBTT (°F)	A302-B DBTT (°F)
0	-220	+15
0.85	-	+245
2.3	+50	+315
9.5	+300	+415

When observing the high DBTT shown in Table 3 it must be kept in mind that these figures are for temperatures less than 450°F. Thus, there is limited recovery due to annealing. In actual application where recovery due to annealing takes place during reactor operation at high temperatures, the DBTT for the pressure vessel steels are considerably lower than those indicated.

As discussed previously, neutron irradiation also increases the yield and tensile strengths of steels. In pure iron, D. Hull and I. L. Mogford found a measurable increase in yield strength with integrated fluxes as low as 1×10^{16} n/cm^2, [3,16]. In alloy steels, however, researchers have determined only a few results for integrated fluxes less than 1×10^{19} n/cm^2. A considerable amount of data is available for fluences in the range 1×10^{19} to 4×10^{19} n/cm^2, and a fair number of results are available for even higher fluences, [3]. Figure 24 shows a plot of how yield strength increases after irradiation at

500°F. This plot is general in nature and mainly conveys an idea of the magnitudes involved. As seen in the figure, there is a rapid increase in yield strength between 1 X 10^{17} and 4 X 10^{17} n/cm^2. This range corresponds reasonably well with the fluence range where there is a large increase in the change in DBTT as previously discussed about Figure 21.

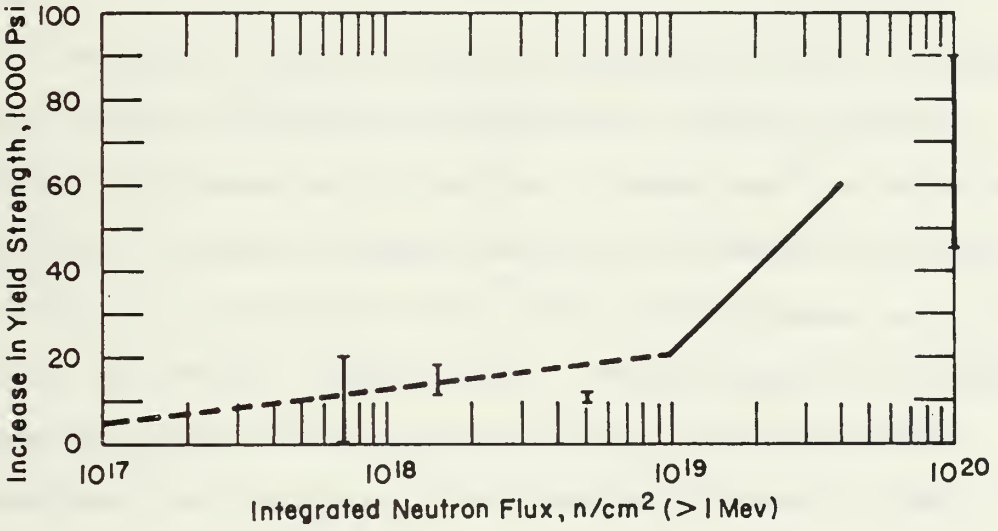

Fig. 24 Yield strength increases of carbon and alloy steels after irradiation at temperatures to 500°F (Ref. [3])

L. P. Trudeau, [3,17], tested HY-80 steel and found yield and tensile strength increases as shown in Table 4 on the next page.

Table 4 Tensile properties of HY-80 steel (Ref. [3,17])

Exposure (n/cm^2)	Irradiation Temp (°F)	Yield strength (10^3 psi)	Tensile strength (10^3 psi)
0	-	103	117
2.5×10^{19}	150	156	161
5×10^{19}	150	176	176

As seen in Table 4, for a fluence of 2.5×10^{19} the yield stength increases by 53,000 psi, and the tensile strength increases by 44,000 psi. These are increases of about 51% in yield strength and 37% for tensile strength. Likewise, at a fluence of 5×10^{19} the increases were 73,000 psi and 59,000 psi respectively. These figures correspond reasonably well with the HY-80 testing results by NRL researchers as reported in NRL Memorandum Report 1808, [15]. Figure 25 shows the tensile properties of HY-80 steel for the indicated irradiation conditions as tested by the NRL. At room temperature, for a fluence of 2.3×10^{19} n/cm^2, Figure 25 shows an increase in yield strength of about 50,000 psi, and an increase in tensile strength of about 33,000 psi. These are increases of about 57% for yield strength and 31% for tensile strength.

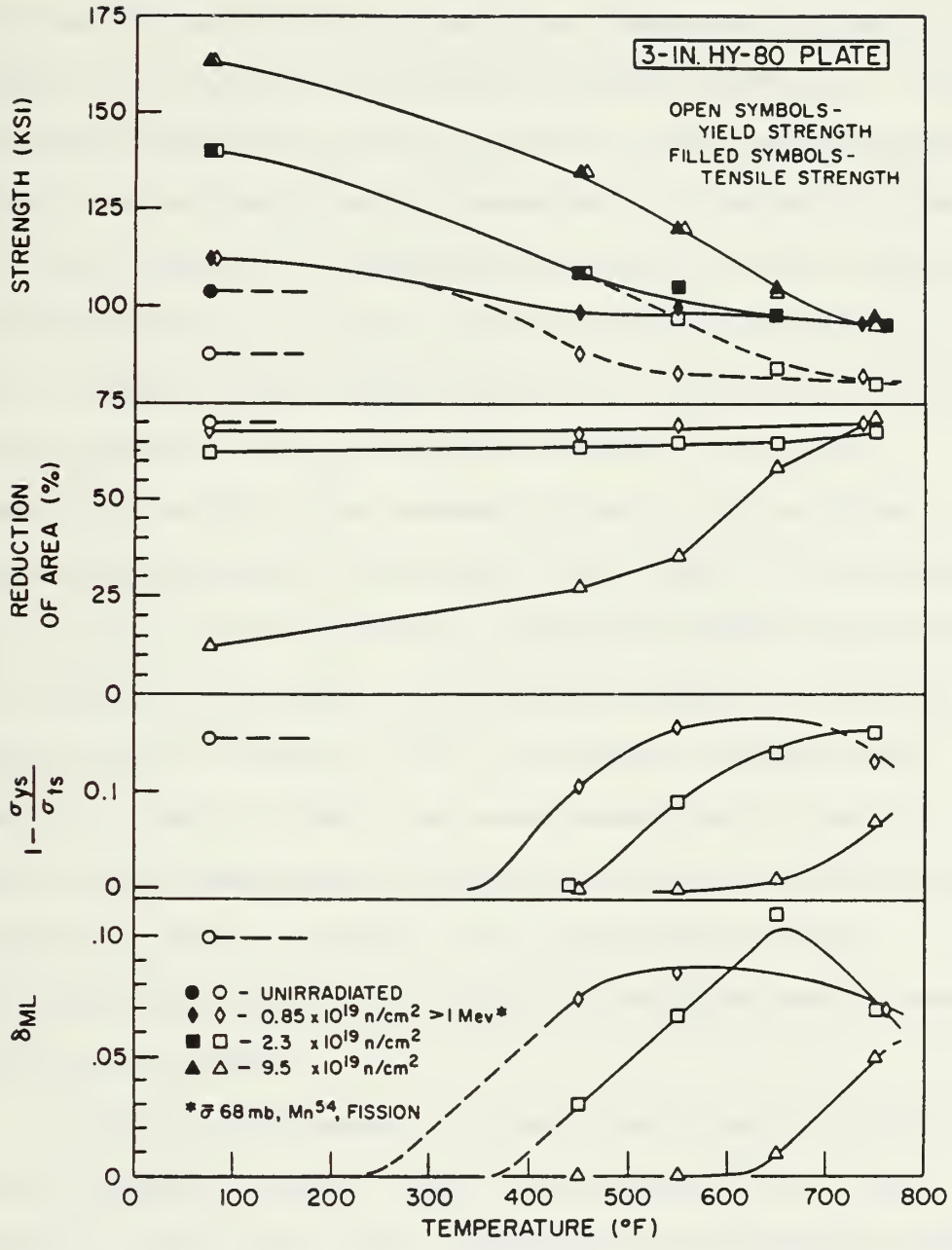

Fig. 25 The tensile properties of HY-80 steel to 750°F for the indicated irradiation conditions (Ref. [15])

Figure 25 also shows the effect on the tensile properties of HY-80 steel at temperatures up to 750°F. It can be seen that as the irradiation temperature rises, the change in the tensile and yield strength decreases. This is due to the annealing effect of the elevated temperatures. At 750° the recovery due to annealing is complete to the point that there is no appreciable change in the yield and tensile strengths from the non-irradiated conditions. In fact, it appears from Figure 25 that in addition to leading to the recovery of the radiation defects, the high temperature of 750° also annealed some of the original manufacturing defects that were in the metal, as evidenced by a slightly lower yield and tensile strength than at the unirradiated conditions. This finding appears at first glance to be in conflict with a previous finding when discussing Table 2 where the same researchers found no recovery of HY-80 steel that was irradiated at 640° and then annealed at 800°F. However, the conditions of the experiments were different, and the two experiments cannot be directly compared.

In 1967, M. Hasegawa of Japan completed the testing of several pressure vessel steels, including HY-80. The results of these tests were reported to the American Society for Testing and Materials (ASTM), and then included in ASTM STP 457, [18]. Hasegawa not only tested U. S. Navy HY-80 steel, but he also tested several Japanese steels that were very similar to HY-80. The symbols and compositions of these steels are shown in Table 5. The symbol SIC3-ASA is

the U. S. Navy HY-80 steel, and the symbol SIC3-ASE is another HY-80 class steel provided to Hasegawa as a reference steel for testing. The other listed symbols represent Japanese steels.

Table 5 Check analyses of HY-80 specimens tested (Ref. [18])

Symbol	Melting	Ingot Weight, kg	Plate Thickness, mm	Check Analysis, percent								
				C	Si	Mn	P	S	Cu	Cr	Mo	Ni
HY-80 FS3-20	B.E.A.F.	10,000	20	0.14	0.23	0.31	0.007	0.005	0.10	1.03	0.32	2.49
YS3-35	B.E.A.F.	2,800	35	0.15	0.14	0.86	0.018	0.010	—	1.54	0.61	4.28
SIC3-ASE (ASTM ref)	B.E.A.F.	—	76	0.14	0.18	0.20	0.011	0.015	0.065	1.61	0.50	3.01
SIC3-ASA (A543)	B.E.A.F.	20,000	203	0.17	0.29	0.38	0.013	0.023	—	1.88	0.51	3.65

The results of Hasegawa's postirradiation tension tests and the shifts in transition temperatures as determined by Charpy V-notch impact tests are summarized in Table 6 and Table 7 respectively on the following page.

Table 6 Results of pre- and postirradiation tension test at room temperature (Ref. [18])

Steel	Symbol of Specimen	Plate Thickness, mm	Conditions of Irradiation		Yield Strength, kg/mm²			Tensile Strength kg/mm²		
			Irradiation Temperature, C	Dosage $\times 10^{19}$ (n/cm², > 1MeV)	Pre-irradiation	Post-irradiation	$\Delta:\sigma_S$ Shift	Pre-irradiation	Post-irradiation	$\Delta:\sigma_B$ Shift
HY-80	FS3-20	20	75 ± 10	2.6	74.0	103.7	+29.7	80.6	104.7	+24.1
	YS3-35	35	75 ± 10	2.6	71.5	102.5	+31.0	88.6	104.6	+16.0

Table 7 Results of pre- and postirradiation Charpy V-notch impact tests (Ref. [18])

Steel	Specimen		Conditions of Irradiation		Tr30 or Tr35, C		
	Symbol	Plate Thickness, mm	Temperature, C	Fluence n/cm² $\times 10^{19}$	Pre-irradiation	Post-irradiation	ΔTr30 or 35
HY-80	FS3-20	20	75 ± 10	3.0	−135	4	+139
	FS3-HS	20	75 ± 10	3.0	−166	−52	+114
	YS3-35	35	75 ± 10	2.9	−54	83	+137
	SIC3-ASE	76	75 ± 10	3.0	−145	63	+208
	SIC3-ASA	203	75 ± 10	3.0	−17	150	+167

The strength figures in Table 6 are given in Kg/mm^2, but these convert to values of psi that compare favorably with previous HY-80 testing results. The change in yield strength for the FS3-20 steel was 42,240 psi, and for the YS-3-35 steel it was 44,090 psi. The change in tensile strength for these two Japanese steels was 34,260 psi and 22,770 psi respectively. As seen previously, the yield strength increases more than the tensile strength, indicating a loss of ductility. These changes correlate to an increase in yield strength of about 40% for the two steels and an increase in tensile strength on the average of about 24%. These relative changes in the strengths are less than those seen by Trudeau or by the NRL researchers, but they do follow the same trends.

Figure 26 shows the increases in DBTT for the HY-80 steels tested by Hasegawa as compared to trends established by researchers at the U. S. NRL and to trends established by G. F. Carpenter, [19]. As can be seen in Figure 26, the reference specimens, SIC3-ASE and SIC3-ASA, fell within the NRL trend bands. It is also clear from the graph that the majority of the Japanese domestic steels were less sensitive to the irradiation than the two U.S. specimens, as evidenced by their smaller change in DBTT, [18].

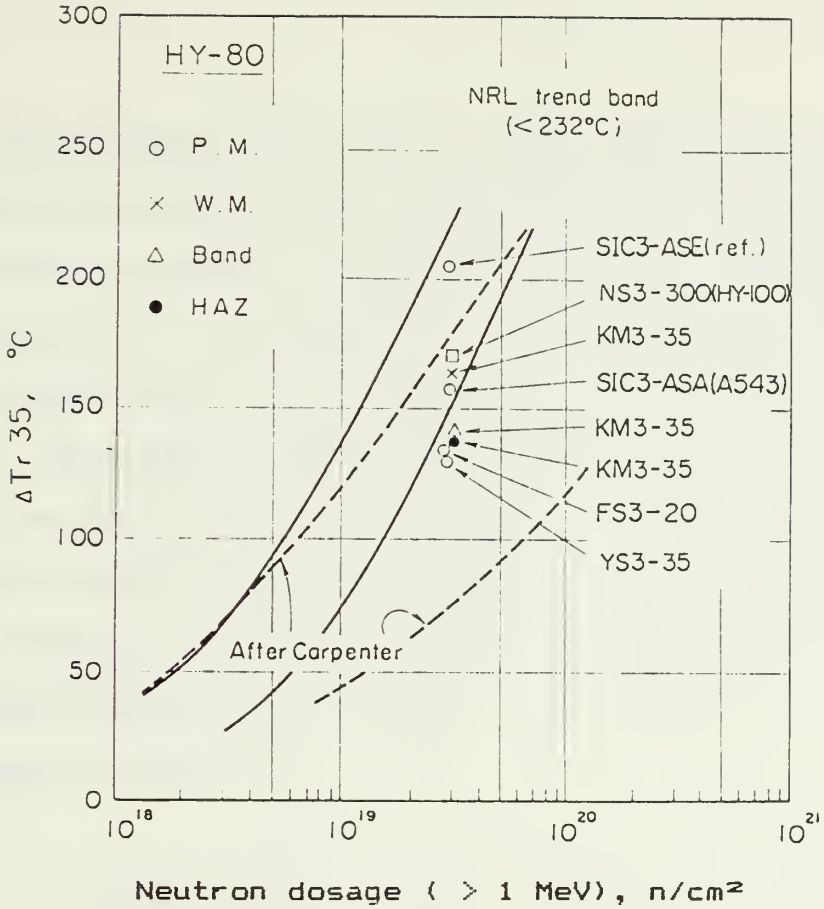

Fig. 26 DBTT changes of HY-80 steels as compared to trends established by NRL and by Carpenter (Ref. [18]

In September 1966 NRL researchers led by L. E. Steele reported in NRL Report 6419 the results of a study done on several higher strength steels, [20]. This NRL report was then included in ASTM STP 426, [21]. Steele and company conducted this testing for two major reasons. First, the ever growing size of nuclear reactors was placing severe demands on the widely used ASTM type A302-B pressure vessel steel - requiring its use in thicknesses of 12 inches or greater for some advanced pressurized-water reactors. Second, the problem of neutron embrittlement with some of the pressure vessel steels in use suggested the desirability

of finding steels which exhibit lower sensitivity, [21]. Although they did not test HY-80 steel in this group, they did test two Ni-Cr-Mo steels, one of which, 3.5Ni-Cr-Mo, is fairly similar in composition to HY-80, and the other, 7.5Ni-Cr-Mo, which is a much higher strength experimental steel. They also tested several other higher strength steels as well as A302-B and A212-B for comparison. The researchers were primarily interested in the results of the Charpy V-notch impact test and the resultant shift in DBTT.

The chemical composition of the two Ni-Cr-Mo steels are shown in Table 8.

Table 8 Chemical composition of 3.5Ni-Cr-Mo and 7.5Ni-Cr-Mo steels (in percent) (Ref. [21])

Element	3.5Ni-Cr-Mo	7.5Ni-Cr-Mo
C	0.17	0.12
Mn	0.38	0.27
Si	0.29	0.21
P	0.013	0.008
S	0.023	0.008
Ni	3.65	7.38
Cr	1.88	0.81
Mo	0.51	0.97
Al	0.02	0.034
N	0.010	---

The initial values of the DBTT, yield strength, and tensile strength of these two steel is shown in Table 9. Representative values for HY-80 steel are also shown for comparison.

Table 9 Mechanical properties of some Ni-Cr-Mo steels (Ref. [21])

Steel	Charpy V DBTT (°F)	Yield strength (KSI)	Tensile strength (KSI)
3.5Ni-Cr-Mo	-130	95.0	122.0
7.5Ni-Cr-Mo	-215	148.8	169.4
HY-80	-145	87.0	105.0

Figure 27 illustrates the Charpy V-notch test results of simultaneous irradiation of the reference A212-B steel and the 7.5Ni-Cr-Mo steel at temperatures below 280°F.

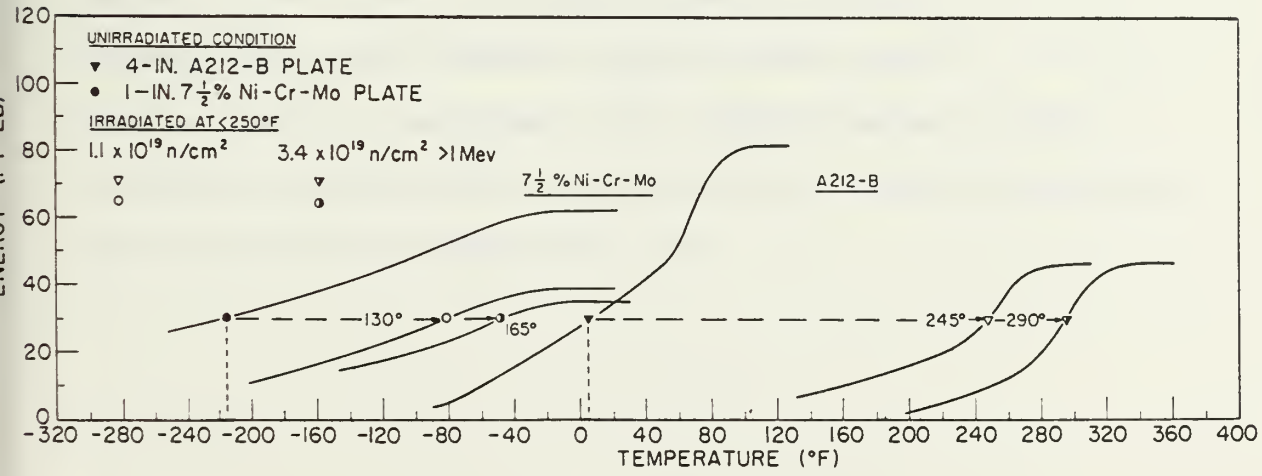

Fig. 27 Charpy V-notch ductility characteristics of the high strength 7.5Ni-Cr-Mo steel before and after irradiations to two neutron exposure levels at a temperature of less than 280°F (Ref. [21])

After simultaneous irradiation to two exposure levels the results of the impact test suggest a much lower sensitivity to radiation embrittlement on the part of the high strength steel when compared with the A212-B steel as seen in Figure 27. Notice also that the transition temperature increase for the high strength steel (165°F after an exposure of 3.4×10^{19} n/cm^2) results in a 30 Ft.Lb. fix point (-50°) which is 55° less than the unirradiated starting point for the A212-B steel and 345° below the as-irradiated transition temperature for the A212-B steel. Noteworthy for both steels are the relatively small increases in transition temperature for the 3.4×10^{19} exposure over that observed for the 1.1×10^{19} exposure. This is a marked indication of radiation damage saturation, [21].

Table 10 shows the comparative embrittlement of these Ni-Cr-Mo steels with the reference steels after irradiation at less than 250°F. Of these steels only the 7.5Ni-Cr-Mo steel showed a significantly lower embrittlement. The others show a DBTT change at both irradiation levels which are so similar that no meaningful differentiation is possible, [21].

Table 10 Comparative embrittlement of several steels irradiated simultaneously at <250°F based on Charpy V-notch tests (Ref. [21])

Steel	Thickness, in.	Initial C_V Value 30-ft-lb, deg F	Experiment A 1.1×10^{19} n/cm²		Experiment B 3.4×10^{19} n/cm²	
			Irradiated Value 30-ft·lb, deg F	ΔT, deg F	Irradiated Value 30-ft·lb, deg F	ΔT, deg F
212-B	4	5	250	245	295	290
302-B	6	30	...	...	...	...
5Ni-Cr-Mo	8	−130	80	210	200	330
5Ni-Cr-Mo	1	−215	−85	130	−50	165

For comparison of embrittlement sensitivity with elevated temperature irradiations, the NRL researchers chose 550°F as the most representative temperature of reactor pressure vessel conditions, and irradiated these high strength steels at 3.8 X 10^{19} n/cm². The results of this irradiation were suggestive of the potential advantage for the higher strength steels. Figure 28 shows the Charpy V-notch characteristics of the two Ni-Cr-Mo steels and A302-B steel. The variation in irradiation embrittlement sensitivity among the three may be compared by the relative upward shift of the individual curves.

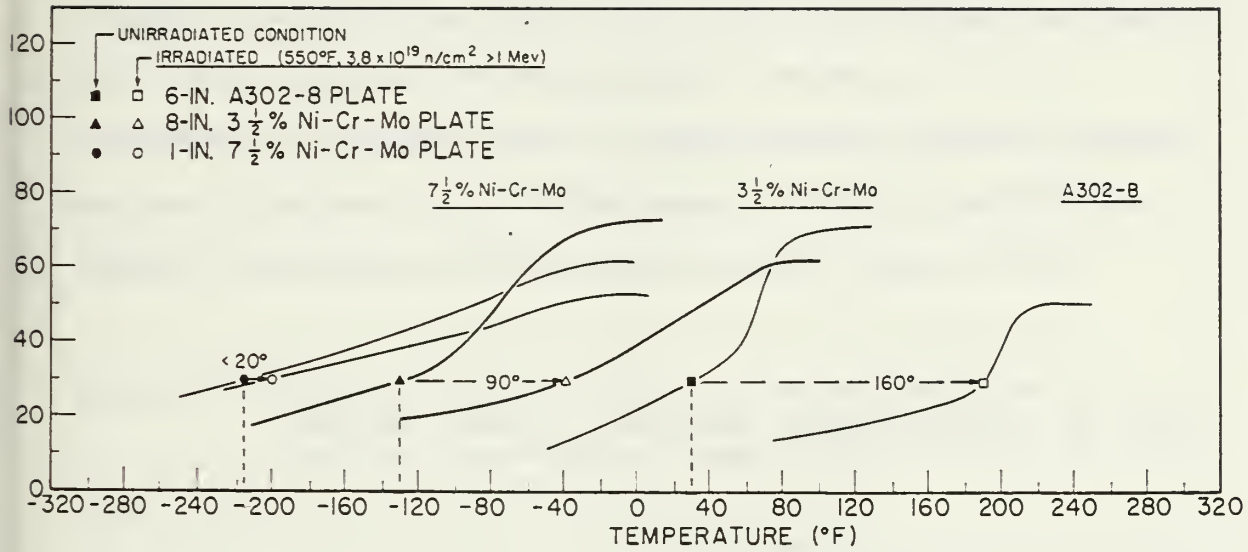

Fig. 28 Charpy V-notch ductility characteristics of three steels of different strength levels after simultaneous irradiations at 550°F (Ref. [21])

Table 11 shows the embrittlement of these Ni-Cr-Mo steels with the reference steels after irradiation at 550°F. The potential advantage of the high strength steels can be measured in terms of both low initial transition temperature and small sensitivity to radiation embrittlement, [21]. The 7.5Ni-Cr-Mo steel shows almost no increase in DBTT. The 3.5Ni-Cr-Mo is more sensitive than the 7.5Ni-Cr-Mo, but again shows a much less transition temperature increase than the A302-B. Additionally, the very low initial DBTT of this steel coupled with the small radiation induced increase results in a DBTT of -40°F after irradiation, which is 70°

below the initial point for the unirradiated A302-B. The NRL researchers point out that when one considers that this exposure temperature of 550° is representative of the operating temperature level of most commercial reactor vessels and that the exposure of 3.8 X 10^{19} n/cm^2 is greater than that expected for most reactor vessels, it is reasonable to assume that the vessel embrittlement problem may be minimized if not eliminated in future reactors by careful selection of the pressure vessel steel, [21].

Table 11 Charpy V-notch ductility characteristics of several steels irradiated simultaneously at 550°F to 3.8 X 10^{19} n/cm^2 (Ref. [21])

Steel	Thickness, in.	30-ft-lb Transition Temperature, deg F		
		Initial	Irradiated	ΔT
12-B	4	5	190	185
02-B	6	30	190	160
Ni-Cr-Mo	8	−130	−40	90
Ni-Cr-Mo	1	−215	−200	15

The NRL researchers, in summarizing their results, made the following comments, [21].

1. The higher strength steels exhibit a general trend toward lower initial NDT.

2. Along with higher strength and lower initial NDT, there is also a tendency for smaller radiation induced increases in transition temperature for the higher strength steels.

3. There appears to be a general tendency for earlier saturation of radiation embrittlement with increasing strength.

4. A marked and progressive advantage in terms of lower radiation embrittlement is observed with the higher strength steels irradiated at 550°F.

In summarizing this section and the previous research done on the mechanical properties of irradiated HY-80 steel the following is noted:

1. Irradiation effects on the mechanical properties of reactor structural materials, including HY-80 steel, do not generally become evident until fluences of over 1 X 10^{18} n/cm^2 have been accumulated.

2. HY-80 and other high strength steels are less sensitive to the effects of neutron irradiation.

3. The unirradiated NDT for HY-80 steel is very low and is on the order of -150°F. After irradiation the shift in the DBTT for HY-80 steel is such that its value is generally less than the unirradiated DBTT for some commonly used pressure vessel steels.

4. After irradiation of about 3 X 10^{19} n/cm^2 the yield strength of HY-80 steel increases around 40-50%, and the tensile strength increases around 20-30%.

5. Ductile-brittle transition temperature shifts of HY-80 steel when irradiated at lower temperatures (<450°F) are on the magnitude of 175°-200°. At elevated temperatures the shift is 75°-100° less.

6. Recovery of irradiated HY-80 steel during annealing is not as complete as that seen in most steels used in pressure vessel construction.

V. EXPERIMENTAL DESCRIPTION AND RESULTS

This section discusses the research conducted by the author on HY-80 steel at the Pennsylvania State University's Breazeale Reactor. The purpose of this research was to determine if lower levels of fast neutron fluence, less than or equal to 1 X 10^{18} n/cm^2, produced measurable changes in the mechanical properties of HY-80 steel when the irradiations and testings were conducted at ambient temperatures. Previous research on the topic has been conducted almost exclusively at fluence levels greater than 1 X 10^{18} n/cm^2 and at elevated temperatures. Very little previous research has conclusively shown that the lower radiation levels produce measurable changes in the tensile strength, hardness, or the impact resistance of this steel. Due to time constraints it was decided to irradiate to two fluence levels. These levels were 5 X 10^{17} n/cm^2 and 1 X 10^{18} n/cm^2. After irradiation, the samples were allowed to decay in order to reduce activity levels. They were then tested to measure the effects the irradiation had on their mechanical properties. The tests performed were the tensile test to determine the yield strength and the ultimate tensile strength, the Charpy V-notch impact test to determine the toughness, and the Rockwell C hardness test to determine hardness.

The discussion is divided into the following subsections:

A. Method

B. Results

C. Discussion of Results

D. Conclusions

A. Method

Three different sample sizes were used - one for tensile testing, one for toughness testing, and one for hardness testing. All specimens were machined from 1" thick HY-80 steel plate utilizing ASTM specifications found in reference [22]. The dimensions for the hardness sample are shown in Figure 29. The tensile specimen specification for a subsize sample was used as shown in Figure 30. The specification for the Charpy V-notch sample is shown in Figure 31 as the Type B specimen.

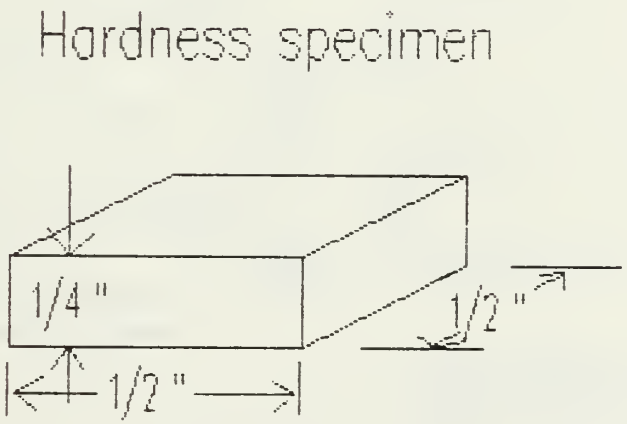

Fig. 29 Dimensions for hardness specimen

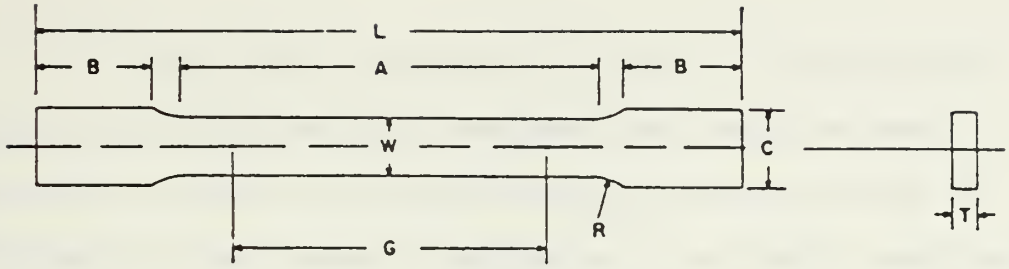

DIMENSIONS

	Standard Specimens				Subsize Specimen	
	Plate-Type, 1½-in. Wide		Sheet-Type, ½-in. Wide		¼-in. Wide	
	in.	mm	in.	mm	in.	mm
G—Gage length (Notes 1 and 2)	8.00 ± 0.01	200 ± 0.25	2.000 ± 0.005	50.0 ± 0.10	1.000 ± 0.003	25.0 ± 0.08
W—Width (Notes 3, 4, and 5)	1½ + ⅛ − ¼	40 + 3 − 6	0.500 ± 0.010	12.5 ± 0.25	0.250 ± 0.002	6.25 ± 0.05
T—Thickness (Note 6)	thickness of material					
R—Radius of fillet, min	½	13	½	13	¼	6
L—Over-all length, min (Notes 2 and 7)	18	450	8	200	4	100
A—Length of reduced section, min	9	225	2¼	60	1¼	32
B—Length of grip section, min (Note 8)	3	75	2	50	1¼	32
C—Width of grip section, approximate (Notes 4, 9, and 10)	2	50	¾	20	⅜	10

Fig. 30 Specifications for tensile specimen (Ref. [22])

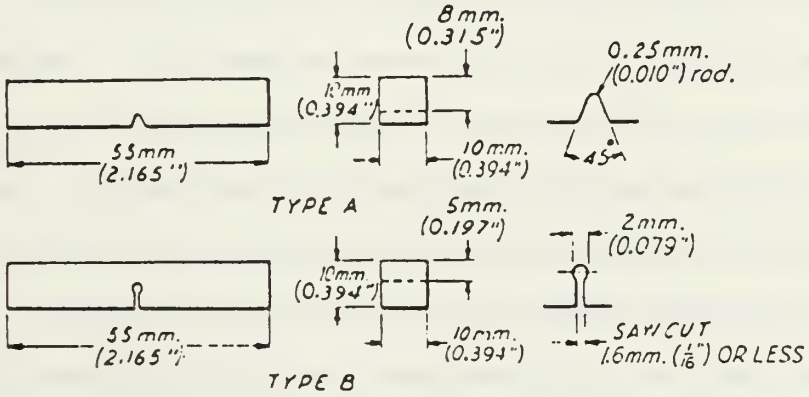

NOTE—Permissible variations shall be as follows:

Adjacent sides shall be at	90 deg ± 10 min
Cross section dimensions	±0.025 mm (0.001 in.)
Length of specimen	+0, −2.5 mm (0.100 in.)
Angle of notch	±1 deg
Radius of notch	±0.025 mm (0.001 in.)
Dimensions to bottom of notch:	
Specimen, Type A	8 ± 0.025 mm (0.315 ± 0.001 in.)
Specimen, Type B	5 ± 0.05 mm (0.197 ± 0.002 in.)
Finish	63 μin. (1.6 μm) max on notched surface and opposite face; 125 μin. (3.2 μm) max on other two surfaces

Fig. 31 Specifications for impact test specimen (Ref. [22])

The subsize specimen was used for the tensile testing, and the hardness specimens were made as small as practical in order to minimize total activity during the experiment. Four tensile specimens, four impact specimens, and two hardness specimens were irradiated at each of the two fluence levels. The ten samples for each fluence level were wired together as compactly as possible in order to receive as uniform a flux as possible within the constraints of the sample irradiation tubes.

Over the course of the experiment the samples were placed within two different sample tubes that were then positioned near the reactor for irradiation. Both sets of samples received their first portion of radiation in a sample tube that was placed on the instrument bridge and then positioned against the core. This tube will be called Tube A. Figure 32 shows a diagram depicting this arrangement. The samples were tied to a string and wire assembly that positioned them in the slot at the bottom of the tube. To achieve the desired neutron spectrum, a thermal shield was placed around and within the tube. The shield reduced thermal neutron and gamma radiation, and allowed predominantly the fast neutrons to pass through and hit the samples. Figure 33 is a more detailed drawing of the lower portion of the tube showing the shielding arrangement.

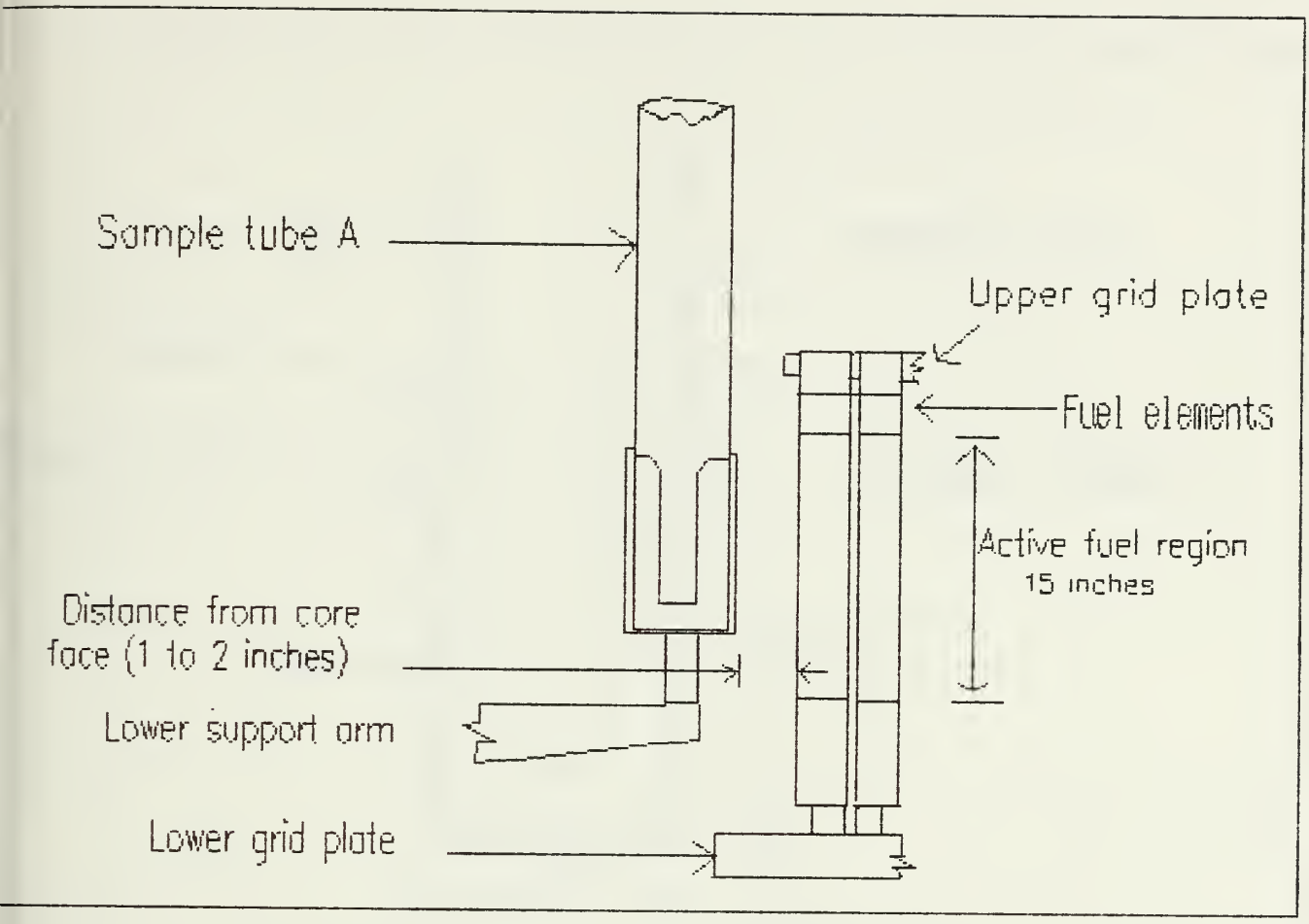

Fig. 32 Tube A irradiation arrangement

The shield includes a cylindrical 2 inch thick by 15 inch high lead gamma ray shield inside the bottom of a 6 1/2 inch diameter aluminum tube. The exterior of the tube is wrapped by a cadmium sheet and a 1/4 inch boral plate to reduce the thermal flux to the order of about 60% of the fast neutron flux, [23]. A shield plug, not shown, is also placed in the tube to provide biological shielding during irradiation of the sample. A CO_2 purge is put in the tube during irradiation to reduce argon 41 generation.

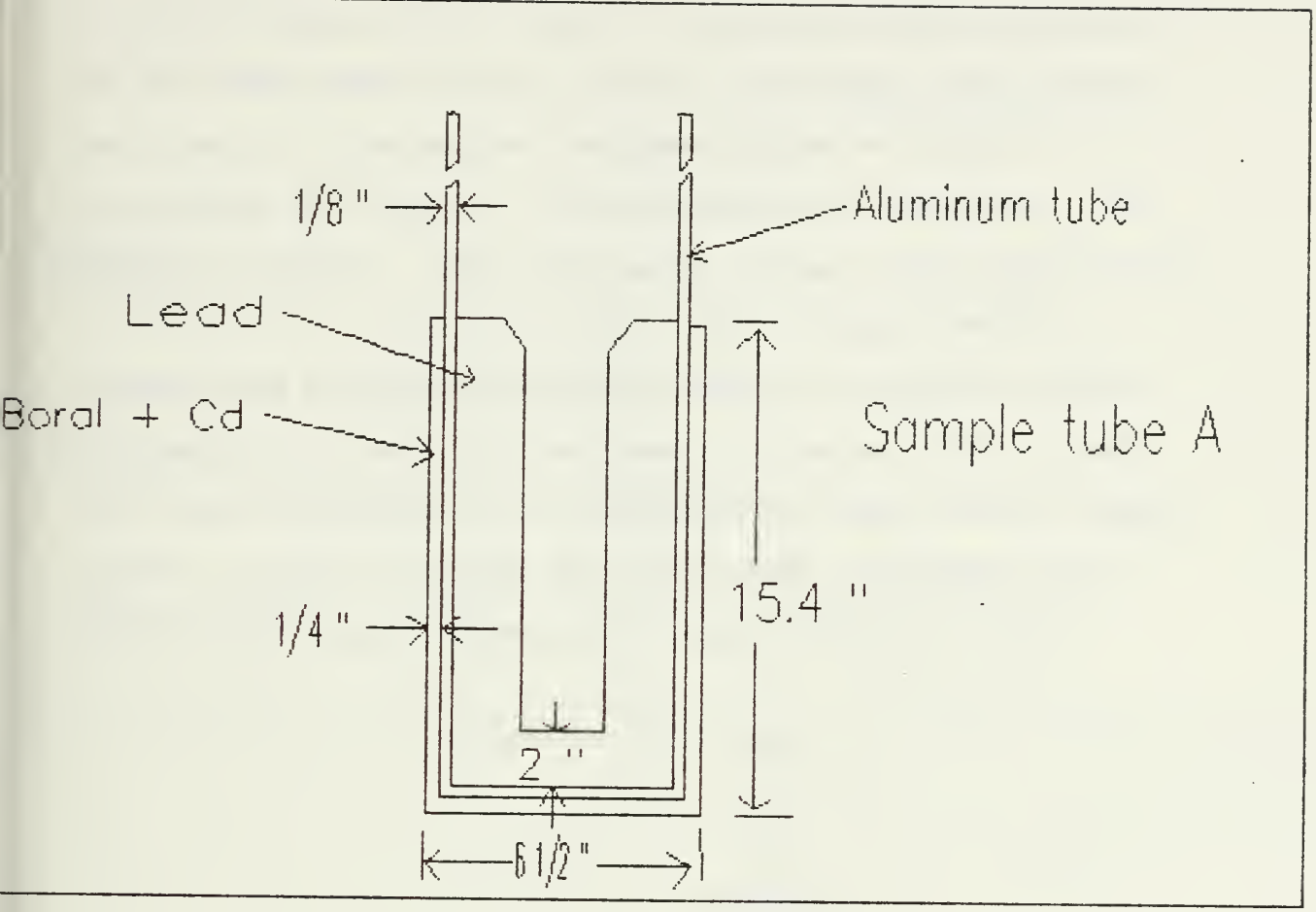

Fig. 33 Tube A shielding design

To reduce the time needed to complete the experiment and to eliminate the need to maintain a CO_2 purge during irradiation, a new sample tube was constructed. This tube will be called Tube B. The remainder of the radiations of both sets of samples was conducted utilizing Tube B. This tube was designed using the same shielding criteria as used in Tube A except for the gamma ray lead shield, which was not included. It was felt that the effects of the gamma rays and of any gamma ray heating would not influence the results of the experiment. Tube B was also designed to be

placed directly on the reactor's lower grid plate instead of on the instrument bridge, thereby simplifying installation. Additionally, the smaller enclosed volume of Tube B eliminated the need for a CO_2 purge during radiation. The design of Tube B, where the major volume of the sample tube is under water with only a small vent through the top, reduced the excessive streaming effect of radiation out of the top of the tube that was seen in Tube A. This allowed for the irradiations to be conducted at higher reactor power levels. Figure 34 shows the irradiation arrangement for Tube B, and Figure 35 shows the basic design of Tube B.

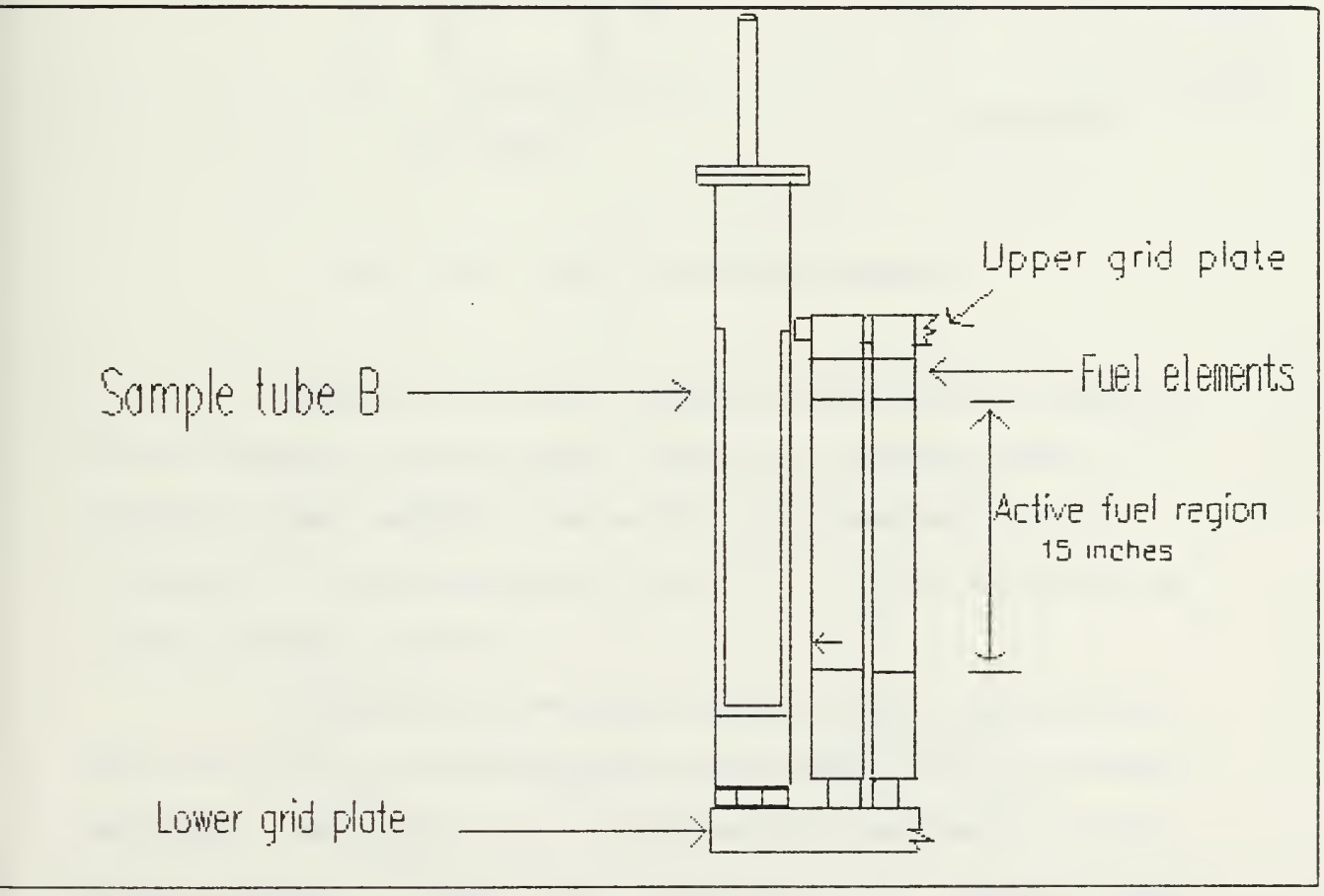

Fig. 34 Tube B irradiation arrangement

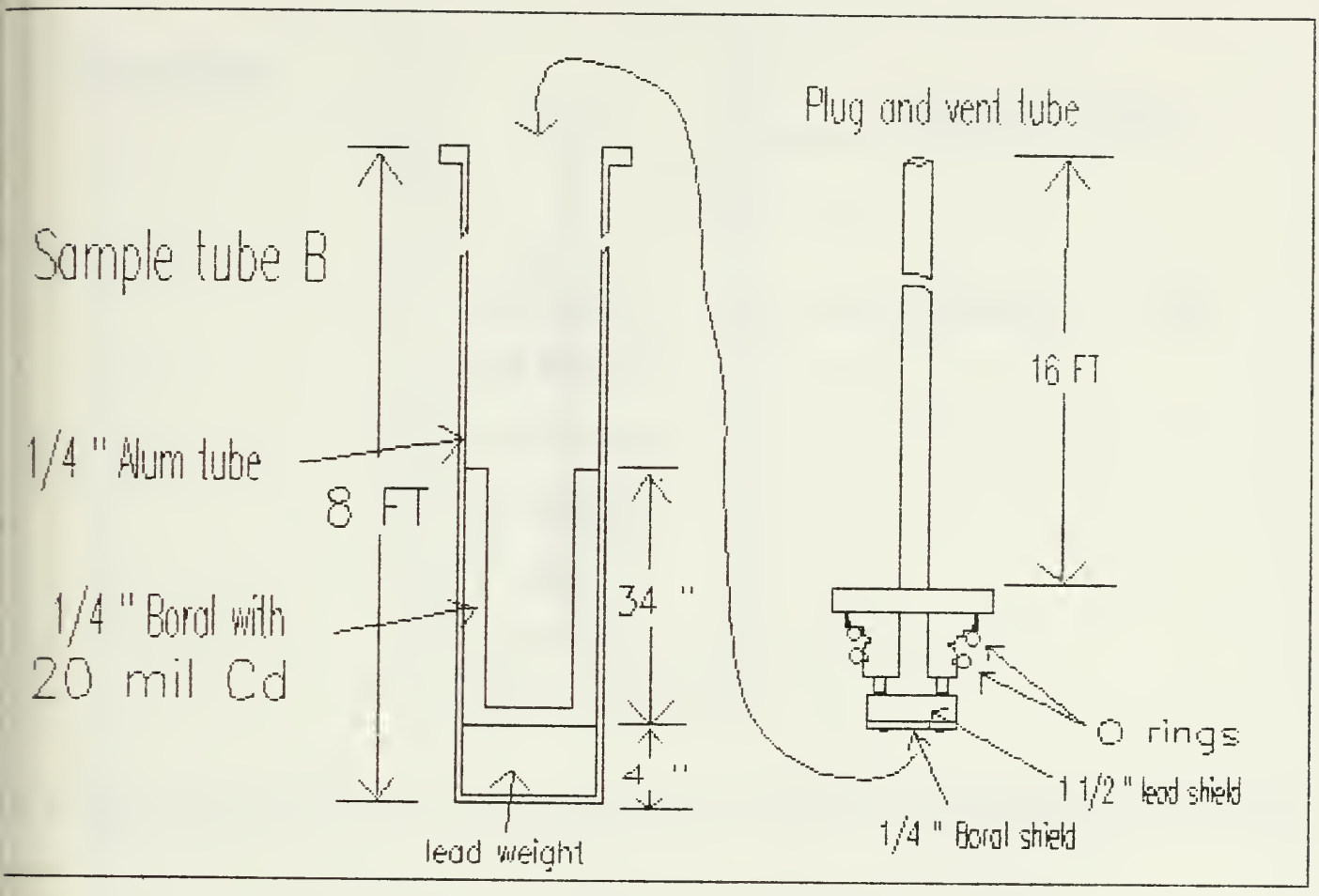

Fig. 35 Tube B shielding design

Based on previous research conducted with Tube A at the reactor, it was known that for a reactor power of 100KW the fast neutron flux within the tube was 1 X 10^{11} n/cm^2-sec. This equates to a flux of 1 X 10^{12} n/cm^2-sec at 1 MW of reactor power.

To determine the fast neutron flux levels within the new tube, flux measurements were taken utilizing sulfur pellets. The pellets were situated near the bottom of the tube as shown in Figure 36. The neutron flux based on the activity of the sulfur pellets is shown in Table 12.

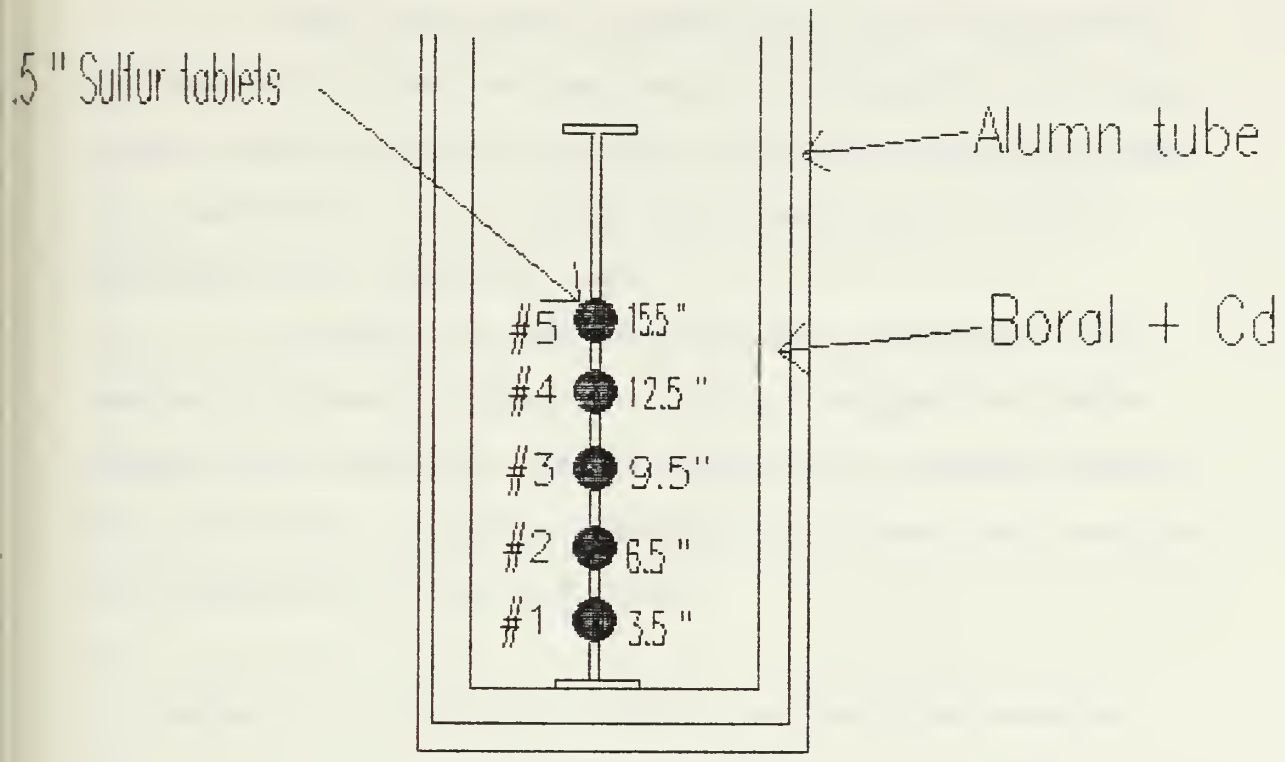

Fig. 36 Sulfur tablet arrangement in Tube B

Table 12 Fast neutron flux in Sample Tube B

Distance from bottom of tube (inches)	Flux at 1 MW (n/cm^2-sec)
3.5	1.4838×10^{13}
6.5	1.7256×10^{13}
9.5	1.6354×10^{13}
12.5	1.2848×10^{13}
15.5	7.896×10^{12}

Since the steel specimens were positioned within the bottom 10 inches of the tube, an average flux for that region was calculated and used to determine the time length of irradiations. The average flux used was 1.6×10^{13} n/cm^2-sec for a power of 1 MW.

A summary of the irradiations conducted on the samples is shown in Table 13. Group 1 samples are those samples that received a total irradiation of approximately 5×10^{17} n/cm^2, and Group 2 samples are those that received an irradiation of 1×10^{18} n/cm^2.

Table 13 Irradiation summary of the HY-80 samples

Tube, Irradiation Time, and Flux	Group 1 Fluences (n/cm^2)	Group 2 Fluences (n/cm^2)
A - 5.36 MWHrs. @ 1×10^{12}	1.9296×10^{16}	1.9296×10^{16}
B - 8.43 MWHrs. @ 1.6×10^{13}	4.85568×10^{17}	4.85568×10^{17}
B - 8.6 MWHrs. @ 1.6×10^{13}	-	4.95136×10^{17}
Total Fast Neutron Fluence Received	5.04864×10^{17}	1.0×10^{18}

Irradiations were completed on 24 July 1986 for the Group 1 specimens, and on 15 August 1986 for the Group 2 specimens. Both sets of samples were then allowed to decay in the reactor pool for at least four weeks prior to any handling or testing.

The machine used for the tensile testing was an Instron Universal Testing Instrument, Floor Model TT-D. The Charpy impact testing machine was a Riehle Precision Impact Tester. The hardness testing machine was a Rockwell Hardness Tester manufactured by the Wilson Mechanical Instrument Company. All testing equipment was properly calibrated and in proper working order except the Riehle Impact Tester. This machine was not routinely used and was not calibrated. However, as long as the machine was consistent, it was felt that the testing results would still show the proper trend in the changes of the material's toughness, even if the actual values were not accurate.

In all three types of testing, several non-irradiated samples were first tested in order to establish the non-irradiated mechanical properties of the HY-80 steel.

During all handling and testing of irradiated specimens, proper radiological controls and procedures were utilized. On 15 October, at the time of testing, the radiation level readings for the individual tensile and impact specimens of Group 2 were approximately .5 mR/Hr. at a distance of 1 foot. The radiation level for the Group 2 hardness specimens was approximately .1 mR/Hr. at 1 foot. The radiation levels for the Group 1 samples were approximately one half the value of the levels of the Group 2 samples.

B. Results

The results of the tensile testing is shown in Table 14. The yield strength was determinied by the .2% offset method. The values shown are the mean values for the number of samples tested. The standard deviation in percentage is also shown.

Table 14 Results of tensile testing

Samples	Yield Strength (psi)	UTS (psi)	% Increase in Yield Strength	% Increase in UTS
Non-irradiated	86,680 (+/- .98%)	103,680 (+/- 1.31%)	-	-
Group 1 (5×10^{17})	90,800 (+/- 1.0%)	107,360 (+/- 1.4%)	4.75	3.55
Group 2 (1×10^{18})	91,360 (+/- 1.47%)	107,820 (+/- 1.74%)	5.4	4.0

The results of the hardness testing is shown in Table 15. All values are Rockwell C (HRC) scale units. The values shown are the mean values for the number of tests conducted on the samples. Also shown is the standard deviation in percentage for each value.

Table 15 Results of hardness testing

Samples	Hardness (HRC)	% Increase in Hardness
Non-irradiated	17.22 (+/- 10.3%)	-
Group 1 (5 X 10^{17})	17.8 (+/- 7.35%)	3.37
Group 2 (1 X 10^{18})	18.57 (+/- 5.8%)	7.87

The results of the Charpy V-notch impact testing is shown in Table 16. Again, the values shown are the mean values for the samples tested with the standard deviation shown in percentage.

Table 16 Results of Charpy V-notch impact testing

Samples	Energy Absorbed (FT.LBS.)	% Decrease of Energy Absorbed
Non-irradiated	27 (+/- 14.3%)	-
Group 1 (5 X 10^{17})	27.25 (+/- 5.5%)	-1.85%
Group 2 (1 X 10^{18})	29.5 (+/- 8.1%)	-9.26%

C. Discussion of Results

In examining the results of the tensile testing as seen in Table 14, a measurable increase in the yield strength and the ultimate tensile strength is apparent. The samples irradiated at 5 X 10^{17} n/cm^2 had an increase of 4.75% in yield strength, and an increase of 3.55% in UTS. The samples iradiated at 1 X 10^{18} n/cm^2 had larger increases in yield strength and UTS of 5.4% and 4.0% respectively. Even when taking into account uncertainties in the figures as shown by the standard deviation, these tests do show a trend of increasing strength with increasing neutron fluence. In both sample groups, the increase in yield strength was greater than the increase in UTS. This change leads to a reduction in the area under the stress-strain curve which is an indication of the material being less tough.

The results of the hardness testing shows a trend of increasing hardness with increasing neutron fluence as seen in Table 15. For the Group 1 samples an increase in hardness of 3.37% was measured, and for the Group 2 samples, an increase in hardness of 7.87% was measured. Because the larger values calculated for the standard deviations in these figures overlap between the non-irradiated and the irradiated samples, the confidence of this accessment is not as high as that for the tensile specimens. However, when coupled with the tensile testing results and considering that hardness changes generally coincide with changes in

tensile strength, the results do tend to indicate a slight increase in hardness.

In examining the Charpy V-notch impact testing results it is first noted that the values determined for the impact resistance are considerably less than would be expected. This was not unexpected because it was known that the testing machine was not in calibration, however, the testing results also do not show the trends that were expected. Previous studies have shown that increasing neutron fluence levels decreases the toughness of a material. The results shown in Table 16 show the opposite trend. For the Group 1 samples, an increase in toughness of 1.85% was measured. For the Group 2 samples, an increase of 9.26% in toughness was measured. As in the hardness testing results, our confidence in these figures is not high due to overlapping standard deviation, but the results still contradict the previous findings. These results lead the author to suspect that either the accuracy of the impact testing machine is not good enough to differentiate any changes that may have been caused by these levels of irradiation, or that there may be some unknown mechanism taking place in the material's microstructure that does produce these contradictory effects at these fluence levels.

D. Conclusions

To conclude the experimental results the following is noted:

1. A fast neutron fluence level of 5×10^{17}

n/cm^2 increased the yield strength of HY-80 steel by 4.75%, and increased its UTS by 3.55%. It also increased its hardness by 3.37%.

2. A fast neutron fluence level of 1×10^{18} n/cm^2 increased the yield strength of HY-80 steel by 5.4%, and increased its UTS by 4.0%. It also increased its hardness by 7.87%.

3. The results of the Charpy V-notch impact testing is considered inconclusive. The results indicate a trend of increasing toughess with increasing neutron fluence vice the expected trend of decreasing toughness, while the tensile test results indicate that the material should be less tough.

4. Although the percentage increases in tensile strength and hardness measured in this research are not high, and the confidence factor for some of the results is low, the trends seen do indicate that fast neutron fluence levels as low as 5×10^{17} n/cm^2 cause measurable changes in the mechanical properties of HY-80 steel.

VI. CONCLUSIONS

Based on the results found in this research and on the results of work by others it is concluded that:

1. The mechanical properties of HY-80 steel, like commonly used pressure vessel steels, are affected by fast neutron radiation.

2. The steel's mechanical properties are affected because of radiation defects, caused by bombarding neutrons initiating collision cascades, that impede or prevent dislocation flow through the material.

3. Previous research has shown that at high irradiation levels on the order of 3×10^{19} n/cm^2 the tensile properties of HY-80 steel can be increased by as much as 50%, and the ductile-brittle transition temperature can be raised by several hundred degrees fahrenheit.

4. Based on the experimental results of this work, fast neutron irradiation levels as low as 5×10^{17} n/cm^2 do cause measurable effects on the mechanical properties of HY-80 steel. These include: increasing the steel's yield strength by 4.75%, increasing its ultimate tensile strength by 3.55%, and increasing its hardness by 3.37%.

References

[1] Phone conversation, Mr. Steel, NAVSEA 08S, and CDR. W. F. Nold, USN, of 18 September 1986.

[2] Orlander, Donald R., Fundamental Aspects of Nuclear Reactor Fuel Elements, TID-26711-P1, Technical Information Center Energy Research and Development Administration, 1976.

[3] Trudeau, L. P., Radiation Effects on Reactor Structural Materials, AEC Monograph Series, American Society for Metals, Rowman and Littlefield, New York, 1964.

[4] Cottrell, A. H., An Introduction to Metallurgy, Edward Arnold Publishers, London, 1967.

[5] Brinkman, J. A., Journal of Applied Physics, 25: 961 (1954).

[6] Seeger, A., "On the Theory of Radiation Damage and Radiation Hardening," Proceedings of the Second United Nations International Conference on the Peaceful Uses of Atomic Energy, Geneva, 1958, Vol. 6, p. 250, United Nations, New York, 1958.

[7] Kinchin G. H., and Pease, R. S., Rep. Progr. Physics., 18:1 (1955).

[8] Bush, Spencer H., Irradiation Effects in Cladding and Structural Material, AEC Monograph Series, American Society for Metals, Rowman and Littlefield, New York, 1965.

[9] Diehl, J. and Seidel, G. P., "Effect of Alloying and Cold Work on the Neutron Irradiation Hardening of Metals," Radiation Damage in Reactor Materials Vol.I, Proceedings of the Symposium on Radiation Damage in Reactor Materials, International Atomic Energy Agency, Vienna, 2-6 June 1969.

[10] Neely, John., Practical Metallurgy and Materials of Industry, John Wiley and Sons, New York, 1979.

[11] Hertzberg, Richard W., Deformation and Fracture Mechanics of Engineering Materials, 2nd Edition, John Wiley and Sons, New York, 1976.

[12] MIL-S-16216J(SH), Military Specification Steel Plate, Alloy, Structural, High Yield Strength (HY-80 and HY-100), 10 April 1981.

[13] Hawthorne, J. R., Steele, L. E., and Pellini, W. S., "Effects of Nuclear Radiation on the Properties of Reactor Structural Materials," NRL Report 5731, Metallurgy Division, U. S. Naval Research Laboratory, Washington, D. C.,. 22 January 1962.

[14] Steele, L. E., and Hawthorne, J. R., "Irradiation Effects on Structural Materials," NRL Memorandum Report 1371, U. S. Naval Research Laboratory, Washington, D. C., November 1962.

[15] Hawthorne, J. R., Serpan, C. Z. Jr., Watson, H. E., Loss, F. J., Potapovs, U., and Klien, E. P., "Irradiation Effects on Reactor Structural Materials," NRL Memorandum Report 1808, Reactor Materials Branch Metallurgy Division, U. S. Naval Research Laboratory, Washington, D. C., 15 August 1967.

[16] Hull, D., and Mogford, I. L., "Precipitation and Irradiation Hardening in Iron," AERE-R 3534, Atomic Energy Research Establishment, Harwell, England, 1960.

[17] Trudeau, L. P., "Irradiation of Some Pressure-Vessel Steels," ASTM STP 2761, American Society for Testing and Materials, 1960, p. 102.

[18] Hasegawa, M., "Irradiation Tests of Several Steels for Reactor Pressure Vessels," Irradiation Effects in Structural Alloys for Thermal and Fast Reactors, ASTM STP 457, American Society for Testing and Materials, 1969, pp. 92-112.

[19] Carpenter, G. F., "Anomalous Embrittling Effects Observed During Irradiation Studies on Pressure Vessel Steels," Nuclear Science and Engineering, Vol. 19, 1964, p. 18.

[20] Steele, L. E., Hawthorne, J. R., and Gray, R. A., "Neutron Irradiation Embrittlement of Several Higher Strength Steels," NRL Report 6419, Reactor Materials Branch Metallurgy Division, U. S. Naval Research Laboratory, Washington, D. C., 7 September 1966.

[21] Steele, L. E., Hawthorne, J. R., and Gray, R. A. Jr., "Neutron Irradiation Embrittlement of Several Higher Strength Steels," Effects of Radiation on Structural Metals, ASTM STP 426, American Society for Testing and Materials, 1967, pp. 346-370.

[22] Metals Test Methods and Analytical Procedures, 1985 Annual Book of ASTM Standards, Section 3, Vol. 03.01, Metals-Mechanical Testing; Elevated and Low-Temperature, American Society for Testing and Materials, Philadelphia, Pa., 1985.

[23] Pao, Yi-Ching, "High Energy Neutron Radiation Damage on Copper", A Thesis in Electrical Engineering, Pennsylvania State University, Department of Electrical Engineering, August 1983.

S

18070 2

DUDLEY KNOX LIBRARY
NAVAL POSTGRADUATE SCHOOL
MONTEREY, CALIFORNIA 93943-5002

220341

Thesis
N842
c.1

Nold
Neutron irradiation effects on the mechanical properties of HY-80 steel.

220341

Thesis
N842
c.1

Nold
Neutron irradiation effects on the mechanical properties of HY-80 steel.

Neutron irradiation effects on the mecha
3 2768 000 70366 4
DUDLEY KNOX LIBRARY c.1